Schymanski, S. J., M. Sivapalan, M. L. Roderick, L. B. Hutley, and J. Beringer (2009), An optimality-based model of the dynamic feedbacks between natural vegetation and the water balance, Water Resour. Res., 45, W01412, doi:10.1029/2008WR006841.

An optimality-based model of the dynamic feedbacks between natural vegetation and the water balance

S. J. Schymanski,[1,2] M. Sivapalan,[3,4] M. L. Roderick,[5] L. B. Hutley,[6] and J. Beringer[7]

Received 16 January 2008; revised 27 August 2008; accepted 7 November 2008; published 15 January 2009.

[1] The hypothesis that vegetation adapts optimally to its environment gives rise to a novel framework for modeling the interactions between vegetation dynamics and the catchment water balance that does not rely on prior knowledge about the vegetation at a particular site. We present a new model based on this framework that includes a multilayered physically based catchment water balance model and an ecophysiological gas exchange and photosynthesis model. The model uses optimization algorithms to find those static and dynamic vegetation properties that would maximize the net carbon profit under given environmental conditions. The model was tested at a savanna site near Howard Springs (Northern Territory, Australia) by comparing the modeled fluxes and vegetation properties with long-term observations at the site. The results suggest that optimality may be a useful way of approaching the prediction and estimation of vegetation cover, rooting depth, and fluxes such as transpiration and CO_2 assimilation in ungauged basins without model calibration.

Citation: Schymanski, S. J., M. Sivapalan, M. L. Roderick, L. B. Hutley, and J. Beringer (2009), An optimality-based model of the dynamic feedbacks between natural vegetation and the water balance, *Water Resour. Res.*, *45*, W01412, doi:10.1029/2008WR006841.

1. Introduction

[2] Natural vegetation has coevolved with its environment over a long period of time and natural selection has resulted in ecosystem structure, function and floristics that are optimally adapted to a given set of environmental conditions [*Givnish*, 1988]. If this were true, the question then arises, what would be the properties of such optimal vegetation and how would it use the available resources? To answer these questions, we propose a vegetation optimality approach to modeling plant function as a result of long-term optimization. In this study, we compare calculated optimal vegetation properties and water use with data describing carbon and water dynamics from a tropical savanna ecosystem. Transpiration is approached from a biological viewpoint, where loss of water through stomata is the inevitable consequence of carbon acquisition by photosynthesis.

[3] Our rationale for this approach is that the energy acquired through photosynthesis is stored in carbohydrates, which are essential for plant survival. Carbohydrates are both energy carriers and building materials for plant organs. They can be used for many purposes, including seed production and the maintenance of symbiotic relations with bacteria and fungi to mobilize nitrogen and other nutrients from the soil or atmosphere. In addition, living plant tissues continuously consume energy to stay alive and require carbohydrates for their construction. Thus, part of the carbon acquired through photosynthesis has to be reinvested into the construction and maintenance of the organs involved in its uptake. Consequently, we assume that only what is left over, the "net carbon profit" (N_{CP}), is useful for increasing a plant's fitness. On this basis we defined the optimal resource use strategy as the one that maximizes N_{CP}.

[4] The organs ultimately involved in carbon uptake are not just leaves, but also roots and transport tissues, which supply the leaves with water and nutrients. For simplicity, the costs related to nutrient uptake were neglected in this study, as they are largely unknown and did not appear to be important for predicting canopy properties and CO_2 uptake rates in a previous study at the same site [*Schymanski et al.*, 2007]. The optimization problem is then to maximize N_{CP} by adjusting foliage properties and stomatal conductivity dynamically, while adapting roots and transport tissues to meet the variable demand for water by the canopy (Figure 1).

[5] The overall modeling approach based on vegetation optimality adopted here was introduced in a previous study [*Schymanski et al.*, 2007], where it was shown that foliage properties and leaf area index of a multilayer canopy could be predicted if water use and vegetation cover were prescribed. A related study showed that the optimal diurnal and day to day dynamics of canopy water use can be calculated if monthly water use and canopy properties are prescribed,

[1]School of Environmental Systems Engineering, University of Western Australia, Crawley, Western Australia, Australia.
[2]Now at Max Planck Institute for Biogeochemistry, Jena, Germany.
[3]Centre for Water Research, University of Western Australia, Crawley, Western Australia, Australia.
[4]Now at Department of Geography and Department of Civil and Environmental Engineering, University of Illinois at Urbana-Champaign, Urbana, Illinois, USA.
[5]Environmental Biology Group, Research School of Biological Sciences and Research School of Earth Sciences, Australian National University, Canberra, ACT, Australia.
[6]School of Science and Primary Industries, Charles Darwin University, Darwin, Northern Territory, Australia.
[7]School of Geography and Environmental Science, Monash University, Clayton, Victoria, Australia.

0043-1397/09/2008WR006841

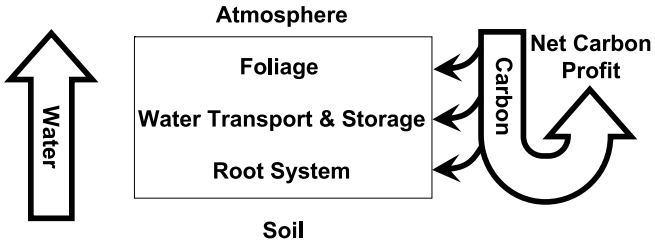

Figure 1. Net carbon profit as the difference between carbon acquired by photosynthesis and the carbon used for the construction and maintenance of organs necessary for its uptake. As CO_2 uptake from the atmosphere is inevitably linked to loss of water from the leaves, the root system as well as water transport and storage tissues are essential to support photosynthesis. The atmosphere (sunlight and water demand) and the soil (water supply) constitute the environmental forcing. Within these constraints, vegetation is assumed to optimize foliage, water transport and storage tissues, roots, and stomata dynamically to maximize its net carbon profit. Figure taken from *Schymanski* [2007] and *Schymanski et al.* [2007].

and that the predicted optimal dynamics corresponded well with observations in a tropical savanna [*Schymanski et al.*, 2008a]. In a subsequent study, a water balance and root water uptake model was introduced, which allowed calculation of the optimal dynamics of root distribution to meet the dynamic canopy water demand, given a prescribed rooting depth [*Schymanski et al.*, 2008b].

[6] The objective of the present study is to eliminate the necessity for prescribing rooting depth, water use or vegetation cover and to allow modeling of the water balance at the diurnal to interdecadal scales, based on abiotic forcing only. To achieve this, the study couples the aboveground and belowground vegetation optimality models and introduces a distinction between a deep-rooted perennial vegetation component (e.g., trees) and a shallow-rooting seasonal vegetation component (e.g., annual grasses). Given meteorology, soil and catchment properties for a tropical savanna site, the adaptable vegetation properties (foliage, stomata and roots) were optimized to achieve a maximum in combined N_{CP} of the perennial and seasonal vegetation components over a 30 year period (1976–2005). The last 5 years of the modeled fluxes were then compared with a 5-year-long record of canopy-scale evapotranspiration and CO_2 flux data [*Beringer et al.*, 2003, 2007; *Hutley et al.*, 2005; *Schymanski et al.*, 2007]. In particular, the model outputs were compared with observations in order to address the following questions: (1) Is the coupled model capable of predicting the annual average evapotranspiration and CO_2 uptake? (2) Can the coupled model predict the seasonality of these fluxes? (3) Does the coupled model predict the correct tree cover and rooting depth as well as the seasonal variation in grass cover? Given that no site-specific information about the vegetation and no calibration are used in the model, one would not normally expect the results to match observations very closely. Alternatively, if one were to find even an approximate correspondence in all the three points outlined above, this would indicate that the chosen objective function (max. N_{CP}) and the constraints (see the methods section below) may qualify as important principles governing the adaptation of natural vegetation to its environment. Such a model would represent a significant advance for hydrological modeling, as the incorporation of the adaptation of natural vegetation to environmental conditions would increase our confidence in long-term predictions of hydrological models, especially in a changing environment.

2. Relation to Existing Optimality-Based Models in Hydrology

[7] A big advantage of optimality-based models is that they reduce the need for model calibration and hence have an increased predictive power compared with conventional models. Process-based models usually have a number of unobservable parameters that need to be calibrated. If such parameters can be assumed to be optimized by the system following a certain goal function, their values do not need to be calibrated but can be calculated a priori. Many parameter sets could lead to the reproduction of various features of the observed data, but the optimality-based model presented here only permits to choose the parameter set which maximizes the objective function, independent of the data match. The data match can then be used independently to assess the model performance.

[8] Optimality principles have been employed by a number of researchers in hydrological or ecological models. Applications include the prediction of optimal root properties [e.g., *Kleidon and Heimann*, 1996, 1998; *van Wijk and Bouten*, 2001; *Laio et al.*, 2006; *Collins and Bras*, 2007; *Guswa*, 2008; *Schymanski et al.*, 2008b], optimal vegetation distributions and structure in semiarid catchments [e.g., *Caylor et al.*, 2004, 2006] and the prediction of optimal photosynthetic canopy properties [e.g., *Evans*, 1993; *Badeck*, 1995; *Dewar*, 1996; *de Pury and Farquhar*, 1997; *Farquhar et al.*, 2002; *Hikosaka*, 2003; *Buckley and Roberts*, 2006; *Schymanski et al.*, 2007; *van der Tol et al.*, 2008a, 2008b].

[9] The idea to use optimality principles in ecohydrology was promoted by Peter Eagleson in the late 1970s and early 1980s [*Eagleson*, 1978, 1982]. Eagleson used two objective functions to derive optimal vegetation properties for a given region, one related to maximising productivity or biomass, and another one to the minimization of plant water stress, the latter of which led him to the conclusion that vegetation should minimize evapotranspiration in order to maximize soil moisture [*Eagleson*, 1978, p. 755]. Recently, *Kerkhoff et al.* [2004] evaluated Eagleson's optimality hypotheses from an ecological perspective and pointed out several inconsistencies with current understanding of vegetation

ecology. Most importantly, the hypothesis that vegetation would have evolved to minimize evapotranspiration has been pointed out to be unrealistic, as this would effectively result in a minimization of photosynthetic activity [*Kerkhoff et al.*, 2004].

[10] Rodriguez-Iturbe and coworkers also assumed that vegetation would minimize "water stress," but, in contrast to Eagleson, they defined water stress quantitatively as a nonlinear function of soil moisture. Different stress functions for grasses and trees were defined on the basis of empirically derived functions of evapotranspiration in relation to soil moisture for both vegetation types. Hypothesizing that individuals in a plant community would act together to reduce their water stress, they showed numerically that spatial interactions between woody and grassy vegetation types can lead to a more efficient community water use, even if both vegetation types compete for the same resource [*Rodriguez-Iturbe et al.*, 1999a, 1999b]. *Rodriguez-Iturbe et al.* [1999a] also showed that the minimum stress condition does not coincide with the maximum productivity condition, which has also been reported by other authors [e.g., *Porporato et al.*, 2001].

[11] Optimality principles have long been used in ecophysiology, for example to make predictions of gas exchange at the leaf scale. *Cowan and Farquhar* [1977] assumed a priori that plants would optimize stomatal conductivity dynamically in order to maximize total photosynthesis for a given amount of transpiration. This assumption, together with a quantitative theory about the nonlinear coupling between transpiration and CO_2 assimilation, allowed them to formulate how stomatal conductivity should vary in response to the rate of photosynthesis and atmospheric water vapor deficit, given a fixed amount of water available for transpiration. This theory, originally derived for the leaf scale, has recently been shown to allow predictions of canopy-scale transpiration [*Schymanski et al.*, 2008a].

[12] In summary, the ecohydrological concept of ecological optimality to date, as described above, was suited for prediction of long-term averages of transpiration only, because of the neglect of the nonlinearity between carbon uptake and transpiration. In contrast, the ecophysiological concept to date, as described above, was suited for the prediction of short-term dynamics only, because of the neglect of the long-term water balance and associated changes in leaf area.

[13] The concept presented in this study combines ecophysiological and ecohydrological optimality approaches. It accounts explicitly for the nonlinear coupling between CO_2 uptake and transpiration, adopting a biochemical model of photosynthesis. At the same time, the presented concept considers the dynamics of soil water and explicit carbon costs of maintaining roots and water transport tissues. This allows modeling gas exchange at smaller temporal scales than the ecohydrological optimality models, and at larger temporal scales than the ecophysiological models mentioned above. Further, the present concept is based on the assumption that N_{CP} (as defined in equation (21)) is maximized by vegetation. This assumption allows formulating a single objective function accounting for both productivity and "water stress," as water stress has a quantifiable impact on carbon uptake by the reduction of stomatal conductivity. The use of a single objective function gives an objective criterion for the choice of a single parameter set from within a large parameter space.

[14] The maximization of N_{CP} is in contrast to the commonly assumed maximization of "net primary production" (NPP) in other optimality-based models [*Raupach*, 2005]. Neither NPP nor N_{CP} are easily observable in nature, as the carbon gained is not necessarily all invested into the buildup of biomass [*Roxburgh et al.*, 2005]. NPP refers to "the rate at which solar energy is stored by plants as organic matter" [*Roxburgh et al.*, 2005], irrespective of whether this energy is subsequently available to the plants or not. In fact, most of the "observable" part of NPP corresponds to energy that is locked up in cellulose and lignin and hence not retrievable by the plants. We believe that maximization of N_{CP} is a more appropriate objective function than the maximization of NPP, because N_{CP} only refers to the energy that is available to the plants for increasing their "biological fitness" (e.g., production of seeds, maintenance of defence mechanisms against pests and herbivores or maintenance of symbiotic relationships to improve nutrient uptake). The growth of new leaves itself could be interpreted as a strategy to increase a plant's "fitness," but here it is merely considered a means to increase the carbon gain. We have to accept that the magnitude of N_{CP} is not measurable itself, but the magnitudes of the fluxes leading up to its calculation are the ones of interest and can be tested against observations, as will be demonstrated in this study.

3. Methods

[15] In this section, we give an overview of the model, while the details can be found in the following subsections. The model code and documentation can also be found at https://projects.bgc-jena.mpg.de/VOM.

[16] Figure 2 illustrates a flow diagram of the model developed in this study. It contains a vegetation model (modified from *Schymanski et al.* [2007, 2008a]) and a water balance model [*Schymanski et al.*, 2008b] providing the belowground conditions for the vegetation model. Both interact mainly by the feedback between root water uptake ($Q_{r,i}$) and soil moisture ($s_{u,i}$). For a model run of 30 years, the model distinguishes between dynamically adapting vegetation properties (at the hourly to daily scale) and slowly adapting vegetation properties that are assumed to be roughly constant during the model run (Table 1). Given the soil water availability calculated by the water balance model, solar irradiance (I_a), atmospheric vapor deficit (D_v), air temperature (T_a) and an initial guess of the constant vegetation parameters, the vegetation optimality model computes the dynamically adapting vegetation properties (vegetated area fraction (M_A), biochemical capacity of the foliage ($J_{\max 25}$), stomatal conductivity (G_s) and root surface area in each soil layer ($S_{Ar,i}$)), their costs and benefits (root respiration (R_r), foliage turnover costs (R_f), water transport costs (R_v) and CO_2 assimilation (A_g)) and the resulting N_{CP}. The optimization algorithm (Shuffled Complex Evolution (SCE)) then searches for the optimal values of the constant vegetation properties (rooting depth and cover of perennial plants ($y_{r,p}$ and $M_{A,p}$ respectively) and the water use parameters $c\lambda_{f,s}$, $c\lambda_{e,p}$, $c\lambda_{f,p}$ and $c\lambda_{e,p}$) that would lead to the maximization of N_{CP} (see section 3.5.1 for details).

[17] Note that only physical catchment properties and climate data enters the model, meaning that no information

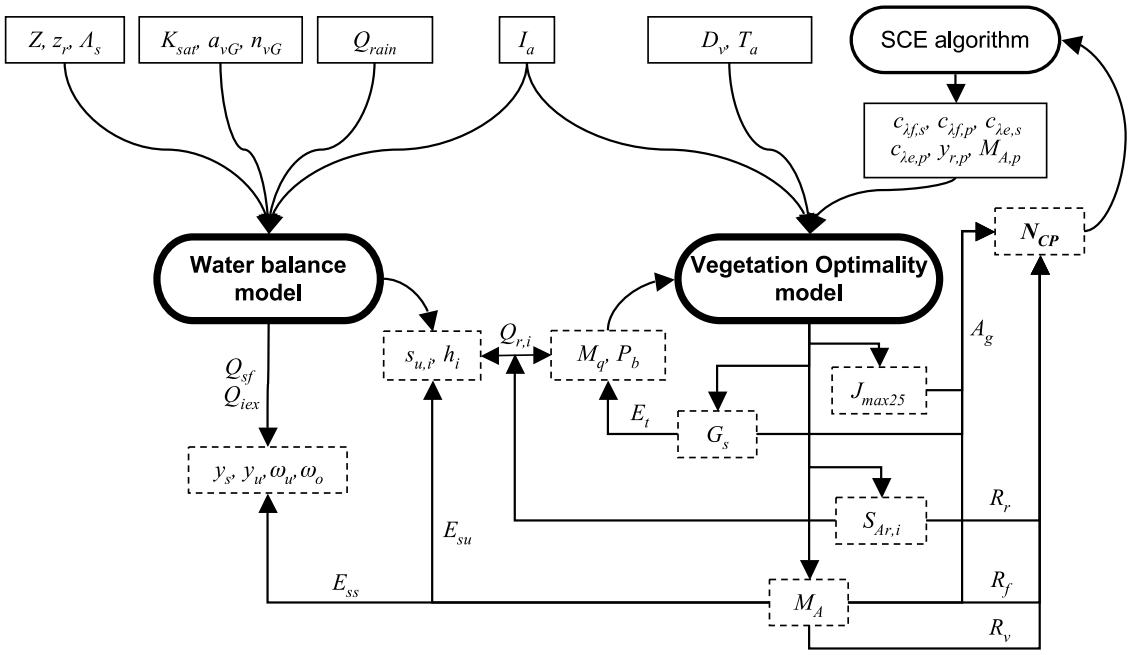

Figure 2. Flow diagram of the coupled water balance and vegetation optimality model. Input variables are at the top, while model outputs are separated into state variables (dashed boxes) and fluxes (along arrows). Symbols are explained in the text (the subscript *i* denotes a vector over all soil layers). For clarity, only selected model outputs are drawn. See the main text for parameter definitions.

about the vegetation at the site is needed and no calibration against the observed fluxes is performed. Only after the SCE algorithm converges to an optimal set of vegetation properties are the CO_2 fluxes and transpiration rates written to a file and compared with the observed fluxes.

3.1. Representation of Vegetation in the Model

[18] Modeling long-term carbon fluxes and water use requires dynamic optimization of the vegetation properties at different time scales (e.g., stomata can adjust at the hourly scale, while rooting depth and vegetation cover can only adjust much more slowly, see Table 1). In addition, dynamic optimization in connection with stochastically varying forcing (e.g., rainfall) is a mathematical challenge in itself, which has not yet been tackled in the ecological optimality context [*Raupach*, 2005] and needs a workaround.

[19] The complexity of the problem made it necessary to further simplify the canopy component and to formulate the optimization problem in terms of a few degrees of freedom. The multilayer canopy model by *Schymanski et al.* [2007] was simplified by neglecting the vertical distribution of light and photosynthetic capacity within the canopy and effectively representing the canopy by means of two "big leaves." One big leaf covering an invariant area fraction ($M_{A,p}$) represented perennial vegetation (e.g., trees) and another big leaf covering a varying area fraction ($M_{A,s}$) represented seasonal vegetation (e.g., annual grasses) (Figure 3). Note that the big-leaf simplification can lead to an overestimation of CO_2 assimilation rates under direct light conditions [*de Pury and Farquhar*, 1997], but this error was considered acceptable in return for computational feasibility of the model. With more powerful computers, this could be relaxed in the future by including the original multilayer canopy model [*Schymanski et al.*, 2007] and optimizing the number of foliage layers and the photosynthetic properties in each layer of the perennial and seasonal vegetation components respectively.

[20] The division of the canopy into two leaves in the model is an allowance for different dynamics and water use strategies by seasonal and perennial plants. As the big

Table 1. Degrees of Freedom (Adjustable Variables) and Time Scales of Variation

Variable	Description	Time Scale of Variation
$y_{r,p}$	thickness of root zone of perennial vegetation	constant over 30 years
$c\lambda_{e,p}$, $c\lambda_{f,p}$	water use parameters of perennial vegetation	constant over 30 years
$c\lambda_{f,s}$, $c\lambda_{e,s}$	water use parameters of seasonal vegetation	constant over 30 years
$M_{A,p}$	fraction of area covered by perennial vegetation	constant over 30 years
$M_{A,s}$	fraction of area covered by seasonal vegetation	varying on daily scale
$J_{\max 25,p}$	electron transport capacity of perennial vegetation	varying on daily scale
$J_{\max 25,s}$	electron transport capacity of seasonal vegetation	varying on daily scale
$S_{Adr,i,p}$	root surface area distribution of perennial vegetation	varying on daily scale
$S_{Adr,i,s}$	root surface area distribution of seasonal vegetation	varying on daily scale
$G_{s,p}$	stomatal conductance of perennial vegetation	varying on hourly scale
$G_{s,s}$	stomatal conductance of seasonal vegetation	varying on hourly scale

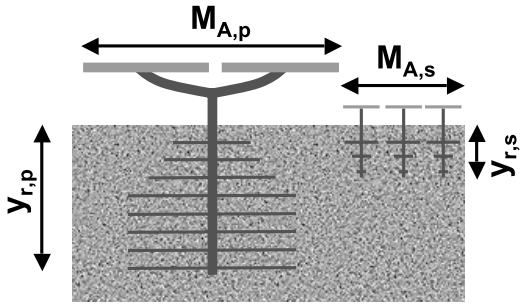

Figure 3. Representation of the (left) perennial and (right) seasonal vegetation components. The perennial vegetation component was assumed to be composed of evergreen trees with a constant cover $M_{A,p}$ and rooting depth $y_{r,p}$, while the seasonal component was assumed to be composed of annual grasses with variable cover $M_{A,s}$ and a rooting depth $y_{r,s}$ limited to 1 m. Note that deep rooting trees need larger vascular systems per unit horizontal cover than shallow rooting annuals.

leaves were not assumed to transmit any light, no overlap between these two leaves was allowed, so that $M_{A,p} + M_{A,s} \leq 1$.

[21] The seasonal component of vegetation was allowed to vary in its spatial extent ($M_{A,s}$), but had a fixed rooting depth ($y_{r,s}$, m) of 1 m, while the perennial component was allowed to optimize its constant rooting depth ($y_{r,p}$, m) without constraints, but had an invariant spatial extent ($M_{A,p}$). The rooting depths were assumed to be invariant in time, but the distribution of roots within each root zone was allowed to vary on a day-by-day basis to account for the fact that root abundance in the soil can be very dynamic and can follow the distribution of soil water [*Schenk*, 2005; *Schymanski et al.*, 2008b]. The biochemical capacity in each "big leaf" was also allowed to vary from day to day, while stomatal conductivity in each "big leaf" was allowed to vary on an hourly scale. The optimized variables and their time scales of variation are summarized in Table 1.

[22] In the following sections, we describe the model from the perspective of the costs and benefits related to the maintenance of the different plant organs necessary for carbon uptake.

3.2. Aboveground Costs and Benefits

[23] In this section, we describe the physiological model that couples light absorption, CO_2 uptake and transpiration in order to quantify the benefits of water use in terms of carbon uptake and the costs of the photosynthetic apparatus in terms of carbon loss due to construction and maintenance.

3.2.1. Photosynthesis

[24] CO_2 assimilation was calculated following a physiological canopy gas exchange model described elsewhere [*Schymanski et al.*, 2007], with the modification that the canopy was represented by two big leaves representing the perennial and seasonal vegetation components, as described above. The gas exchanges of the perennial and seasonal vegetation components were modeled independently as a function of their respective electron transport rates and stomatal conductivities. Following *Schymanski et al.* [2007], differences between the photosynthetic pathways of C3 and C4 plants were neglected and all plants were modeled as C3 plants. The increased uncertainty due to this ignorance about the dominant photosynthetic pathway was accepted in return for greater generality.

[25] The functional dependence of CO_2 uptake rate (A_g, mol s^{-1} m^{-2}) on photosynthetic active irradiance (I_a, mol s^{-1} m^{-2}), electron transport rate (J_e, mol s^{-1} m^{-2}), stomatal conductivity (G_s, mol s^{-1} m^{-2}), air temperature (T_a, K) and the mole fraction of CO_2 in the air (C_a, mol mol^{-1}) is summarized in the following equations [*Schymanski et al.*, 2007]:

$$A_g = \frac{1}{8}\Big(4C_aG_s + 8\Gamma_*G_s + \Big(\big(J_e - 4R_l - 4G_s\big(C_a - 2\Gamma_*\big)\big)^2 + 16G_s(8C_aG_s + J_e + 8R_l)\Gamma_*\Big)^{\frac{1}{2}}\Big) \quad (1)$$

where Γ_* (mol mol^{-1}) is the CO_2 compensation point in the absence of mitochondrial respiration, which is fairly constant between plant species, but varies with temperature [*Medlyn et al.*, 2002]. The electron transport rate (J_e) is a function of irradiance (I_a), the big leaf's electron transport capacity (J_{max}, mol s^{-1} m^{-2}) and the area fraction covered by the leaf (M_A):

$$J_e = \Big(1 - e^{-\frac{0.3I_a}{J_{max}}}\Big)J_{max}M_A \quad (2)$$

while the leaf respiration rate (R_l, mol s^{-1} m^{-2}) is determined by (J_{max}):

$$R_l = \frac{M_A c_{Rl} J_{max}\big(C_a - \Gamma_*\big)}{8\big(C_a + 2\Gamma_*\big)} \quad (3)$$

The parameter c_{Rl} is a constant with an assigned value of 0.07, following an empirical relationship between photosynthetic capacity and leaf respiration [*Givnish*, 1988; *Schymanski et al.*, 2007].

[26] The temperature dependencies of Γ_* and J_{max} were modeled empirically [*Medlyn et al.*, 2002], where we assumed that leaf temperature is the same as air temperature. Equation 12 of *Medlyn et al.* [2002] was used for the temperature dependence of Γ_* after converting it to the International System of Units (SI). Parameter values given for *Eucalyptus pauciflora* were used for the temperature dependence of J_{max}, given its reference value at 25°C (J_{max25}, mol s^{-1} m^{-2}). Of these parameter values, only the "optimal temperature" of the response function was modified and set to 305 K to reflect the site's mean air temperature.

[27] Equations (1) to (3) were applied to both the seasonal and perennial vegetation components, with different sets of values for M_A, J_{max25} and G_s. The total vegetation net CO_2 uptake rate ($A_{g,tot}$, mol s^{-1} m^{-2}) was calculated as the sum of net CO_2 assimilation by perennial ($A_{g,p}$) and by seasonal plants ($A_{g,s}$):

$$A_{g,tot} = A_{g,p} + A_{g,s} \quad (4)$$

3.2.2. Stomatal Conductivity and Transpiration Rate

[28] Transpiration (E_t, mol s^{-1} m^{-2}) was modeled as a diffusive process, where the stomatal conductivity for CO_2

(G_s, mol s^{-1} m^{-2}) was multiplied by a constant (a = 1.6) to account for the different diffusivities of water vapor and CO_2 in air [*Cowan and Farquhar*, 1977]:

$$E_t = aG_s(W_l - W_a) \tag{5}$$

W_l and W_a denote the mole fraction of water vapor in air inside the leaf and in the atmosphere respectively. The mole fraction of water vapor in air was estimated by dividing the partial vapor pressure (p_{va}, Pa) by air pressure (P_a, Pa). Assuming that the air space inside the leaves is saturated (with partial vapor pressure p_{vsat}) and that leaf temperature equals air temperature (T_a), we approximated the term (W_l–W_a) by the molar vapor deficit (D_v):

$$W_l - W_a \approx \frac{p_{vsat} - p_{va}}{P_a} = D_v \tag{6}$$

where p_{vsat} denotes the saturated vapor pressure and was calculated using equation (A5).

[29] Note that leaf temperatures can be 1.5–2° above air temperature at the study site (L. D. Prior, personal communication, 2005), which means that the assumption of equal leaf and air temperatures would lead to an underestimation of D_v. On the other hand, the air space inside the leaves is likely less than saturated [*Canny and Huang*, 2006], which would result in an overestimation of D_v using the above method. We conclude that the effects of the two simplifying assumptions of equal air and leaf temperatures and saturated vapor pressure inside the leaf could partly negate each other.

3.2.3. Carbon Costs Related to the Photosynthetic Apparatus

[30] The leaf respiration rate (R_l) was formulated above as a function of the leaf's photosynthetic capacity (equation (3)). This formulation implies that the maintenance of infrastructure to perform photosynthesis has an associated cost, which can be expressed as the expenditure of carbon for respiration. More generally, respiration can be seen as a result of active processes, which includes the synthesis of proteins and structural dry matter, but also, for example, nutrient conversions, ion transport or phloem loading [*Dewar*, 2000]. What is generally referred to as "maintenance respiration" could be thought of as the respiration resulting from the active processes counteracting natural decay. Extending this further, we formulate "maintenance costs" as the carbon that has to be invested to negate the decay rates of certain structures. These can also include the carbon that, for example, is lost because of litter fall.

[31] It is obvious from equation (2) that a larger vegetated fraction (M_A) leads to larger electron transport rates (J_e), which would result in larger CO_2 uptake rates. However, leaves have limited life times, so that the plants need to invest carbon into the replacement of fallen leaves. It has been shown that these turnover costs can be estimated to be equivalent to an average carbon investment of 0.22 μmol s^{-1} m^{-2} leaf area [*Schymanski et al.*, 2007]. In order to relate M_A to leaf area, we assumed that the clumped leaf area index within vegetated patches is 2.5 [*Schymanski et al.*, 2007], so the carbon costs related to leaf area were approximated as:

$$R_f = 2.5 \times 0.22\ \mu\text{mols}^{-1}\text{m}^{-2}M_A = 5.5 \times 10^{-7}\text{mols}^{-1}m^{-2}M_A \tag{7}$$

3.3. Water Balance and Belowground Costs

[32] The canopy water demand has to be met by root water uptake below ground, which incurs additional costs. A previous study presented a coupled water balance and root water uptake model that allowed the calculation of these costs for given canopy water demand, climate and catchment properties [*Schymanski et al.*, 2008b]. This model was used in the present study with just a few alterations to make it compatible with the aboveground part and to further speed up the calculations. In the following sections, the model and the alterations used here will be described briefly, while the details about the model can be found elsewhere [*Schymanski*, 2007; *Schymanski et al.*, 2008b].

3.3.1. Root Water Uptake

[33] Following *Schymanski et al.* [2008b], roots were assumed to withdraw water from the unsaturated zone only, which was subdivided into consecutive layers of thickness $\delta_{yu,i}$ (m) each, where i is an index starting with 1 at the soil surface. Root water uptake was modeled using an electrical circuit analogy, where the driving force is the difference between the forces holding the water in the soil (h_i, m head) and the forces holding the water in the roots ($h_{r,i}$, m head). Radial root resistivity (Ω_r, s) and soil resistivity ($\Omega_{s,i}$, s) were in series in each soil layer [*Schymanski et al.*, 2008b]:

$$Q_{r,i} = S_{Ar,i}\left(\frac{h_{r,i} - h_i}{\Omega_r + \Omega_{s,i}}\right) \tag{8}$$

where $S_{Ar,i}$ (m^2 m^{-2}) is the root surface area per ground area in layer i. The resistivity of the soil to water flow toward the roots ($\Omega_{s,i}$, s) was formulated as a function of the unsaturated hydraulic conductivity in the soil ($K_{unsat,i}$, m s^{-1}), root radius (r_r, m) and root surface area density in soil layer i ($S_{Adr,i}$, m^2 m^{-3}) [*Schymanski et al.*, 2008b]:

$$\Omega_{s,i} = \frac{1}{K_{unsat,i}}\sqrt{\frac{\pi r_r}{2S_{Adr,i}}} \tag{9}$$

[34] Root suction head ($h_{r,i}$, m) was expressed as a function of tissue balance pressure above ground (P_b, bar) and the hydrostatic head between the soil surface and soil layer i ($h_{h,i}$, m):

$$h_{r,i} = c_{Pbm}P_b - h_{h,i} \tag{10}$$

where c_{Pbm} = 10.2 m bar^{-1} is a conversion coefficient to convert from units of P_b (bar) to units of $h_{r,i}$ (m). The height of the canopy was not considered in the calculation of $h_{h,i}$, as it was not modeled.

[35] For the seasonal plants, $P_{b,s}$ was set to a constant value of 15 bars, while for trees, $P_{b,p}$ was modeled as a function of aboveground dry matter in living tissues (M_d, kg m^{-2}), water storage capacity of living tissues (M_{qx}, kg m^{-2}) and the variable tree water store (M_q, kg m^{-2}) per unit catchment area [*Schymanski*, 2007; *Schymanski et al.*, 2008b]:

$$P_{b,p} = \left(M_{qx} - M_q\right)\left(\frac{c_1 M_d}{\left(M_d + M_{qx}\right)^2} + \frac{c_2}{M_{qx}}\right) \tag{11}$$

where c_1 (750 bar) and c_2 (1 bar) are constants found to represent a large variety of plants [*Roderick and Canny*, 2005; *Schymanski*, 2007].

[36] To get a rough estimate of realistic values for M_{qx} and M_d per unit vegetated area, we used observations at the study site. *Cernusak et al.* [2006] measured specific leaf area at the study site as 5.5 m^2 kg^{-1}, so with a leaf area index of 0.7 in the dry season, this would result in 0.127 kg of dry matter in the foliage per m^2 catchment area. *Cernusak et al.* [2006] also estimated the total aboveground volume of sapwood at the site to be 0.0032 m^3 per m^2 catchment area and observed mean values of sapwood density varying between species from 0.81 to 0.94 g cm^{-3}. In rough terms, this would give an estimate of 3 kg sapwood dry matter per m^2 catchment area, or, using our estimate that 30% of the area was covered by trees, the amount of sapwood dry matter per m^2 area covered by trees was 10 kg. On the basis of these considerations, we expressed the total living tissue dry matter per m^2 catchment area (M_d) as a function of the area fraction covered by trees ($M_{A,p}$):

$$M_d = 10 \text{ kgm}^{-2} M_{A,p} \tag{12}$$

Knowing that the vegetation at the site experiences periods with low soil moisture, we set $M_{qx} = M_d$ in the present model, as this setting allows the maximal values of P_b in equation (11). It is also consistent with values typically found in eucalypt leaves by *Roderick and Canny* [2005].

3.3.2. Root Maintenance Costs

[37] As in the case of leaves, root longevity seems to be generally related to tissue density and root diameter, but the small range of data currently available does not allow us to model root life span as a function of particular root properties [*Eissenstat and Yanai*, 1997; *Eissenstat et al.*, 2000].

[38] In the absence of a more general theory of root maintenance costs, we followed the same approach as in the work by *Schymanski et al.* [2008b] where the relation between the roots' water extraction capacity and their maintenance costs was derived from measurements on citrus fine roots. The parameterization derived by *Schymanski et al.* [2008b] is summarized below.

[39] The resistivity of fine roots to water uptake (Ω_r, s) was set to [*Schymanski et al.*, 2008b]:

$$\Omega_r = 1.02 \times 10^8 \text{s} \tag{13}$$

Root respiration per unit catchment area (R_r, mol s^{-1} m^{-2}) as a function of root radius (r_r, m) and root surface area per unit ground area (S_{Ar}, m^2 m^{-2}) was calculated as:

$$R_r = c_{Rr}\left(\frac{r_r}{2} S_{Ar}\right) \tag{14}$$

where $c_{Rr} = 0.0017$ mol s^{-1} m^{-3} and $r_r = 0.3 \times 10^{-3}$ m for citrus fine roots [*Schymanski et al.*, 2008b].

3.3.3. Water Balance Model

[40] In the above, root water uptake rates were formulated as a function of the matric suction head (h_i, m) and unsaturated hydraulic conductivity ($K_{unsat,i}$, m s^{-1}) in each soil layer. These can be calculated using a variety of water balance models and the one used here has been described in detail by *Schymanski* [2007] and *Schymanski et al.* [2008b]. It is based on the spatially lumped "representative elementary watershed" (REW) concept by *Reggiani et al.* [2000], with an added vertical resolution of the unsaturated zone into layers of thickness δ_{yu} (m). To reduce computation time, δ_{yu} was increased to 0.5 m, compared with the value of 0.1 m given by *Schymanski et al.* [2008b]. The topographical catchment properties needed for the model were the average depth of the pedosphere (Z, m), the average elevation of drainage channels with respect to the average bedrock elevation (z_r, m) and the average slope angle of the seepage face (γ_0). Water fluxes between different soil layers were calculated using a discretization of the Buckingham-Darcy equation [*Radcliffe and Rasmussen*, 2002], which is the 1-D equivalent to Richards' equation for steady flow. Runoff was calculated as a function of the physical catchment properties and the thickness of the saturated zone, which varied because of water exchange with the unsaturated zone and across the seepage face. Runoff routing was not included in the model, so that all outflow from the saturated zone and infiltration excess was assumed to be immediate runoff. Runoff routing and feedbacks between neighboring REWs could be included in the future, if desired.

[41] The matric suction head (h_i, m) and unsaturated hydraulic conductivity ($K_{unsat,i}$, m s^{-1}) in each soil layer were calculated as a function of the soil saturation degree ($s_{u,i}$) following the widely used water retention model by *van Genuchten* [1980]:

$$h_i = \frac{1}{\alpha_{vG}}\left(s_{u,i}^{-\frac{1}{m_{vG}}} - 1\right)^{\frac{1}{n_{vG}}} \tag{15}$$

where α_{vG}, n_{vG} and m_{vG} are constants specific to soil type, where n_{vG} and m_{vG} are assumed to follow the relation:

$$m_{vG} = 1 - \frac{1}{n_{vG}} \tag{16}$$

The unsaturated hydraulic conductivity (K_{unsat}, m s^{-1}) was expressed as a function of soil moisture and the saturated hydraulic conductivity (K_{sat}, m s^{-1}) [*van Genuchten*, 1980]:

$$K_{unsat} = K_{sat}\sqrt{s_u}\left(1 - \left(1 - s_u^{\frac{1}{m_{vG}}}\right)^{m_{vG}}\right)^2 \tag{17}$$

The parameter values of K_{sat}, α_{vg}, n_{vG} and the soil porosity needed for the water balance model (the parameter ε (m^3 m^{-3}) given by *Schymanski et al.* [2008b]) were taken from the software package Hydrus 1-D [*Simunek et al.*, 2005] as typical values given for sandy loam ($K_{sat} = 1.23 \times 10^{-5}$ m s^{-1}, $\alpha_{vg} = 7.5$ m^{-1}, $n_{vG} = 1.89$, $\varepsilon = 0.345$ m^3 m^{-3}).

[42] In the current study, the water balance was calculated for a period of 30 years, for which no data on soil temperature was available. Therefore, soil evaporation (E_{su} and E_{ss} for the unsaturated and saturated surface area fractions respectively, in units of m^3 m^{-2} s^{-1} = m s^{-1}) was simulated as a function of the saturation degree in the top soil layer ($s_{u,1}$), and the amount of global radiation (I_g, W m^{-2}) that reaches the soil:

$$E_{su} = \frac{I_g\left(1 - 0.8\left(1 - M_{A,tot}\right)\right)\omega_u s_{u,1}}{\lambda_E \rho_w} \tag{18}$$

and

$$E_{ss} = \frac{I_g\left(1 - 0.8\left(1 - M_{A,tot}\right)\right)\omega_o}{\lambda_E \rho_w} \tag{19}$$

where $M_{A,tot}$ is the vegetated fraction of the surface ($M_{A,tot} = M_{A,p} + M_{A,s}$), ω_u and ω_o are the unsaturated and saturated surface fractions respectively, $\lambda_E = 2.45 \times 10^6$ J kg^{-1} is the latent heat of vaporization and $\rho_w = 1000$ kg m^{-3} is the density of liquid water.

3.3.4. Water Transport Costs

[43] Water that is taken up by fine roots needs to be transported to leaves where it is transpired. The vascular system required for this transport is most obvious in the stems and branches of trees. An equivalent structure is needed below ground, so that we expect that deeper root systems and larger crown areas require larger vascular systems (Figure 3). These structures are expected to have specific decay rates, but unlike the case for leaf area, a relationship between size and carbon costs could not be derived from the literature. Therefore, we assumed that the carbon costs related to the maintenance of the vascular system (R_v, mol s^{-1} m^{-2}) are a linear function of rooting depth (y_r, m) and the horizontal extent of the vegetation (M_A):

$$R_v = c_{rv} M_A y_r \tag{20}$$

where c_{rv} (mol m^{-3} s^{-1}) is an unknown proportionality constant, which had to be tuned as described in section 4. Note that R_v should also increase with the canopy height, but since the canopy height was not modeled here this effect was not included. The quantification of the costs and benefits of canopy height and its inclusion in the optimization scheme is left for future work.

3.4. Objective Function

[44] Following the concept of vegetation optimality, as described above, the objective function for the optimization was taken as the maximization of N_{CP}, defined as total CO_2 uptake of perennial and seasonal plants over the entire period, minus all identified maintenance costs of the organs assisting photosynthesis, including foliage, roots and water transport tissues:

$$N_{CP} = \int \left(A_{g,tot}(t) - R_f(t) - R_r(t) - R_v(t)\right) dt \tag{21}$$

where $A_{g,tot}$ (see equation (4)) is the CO_2 assimilation by all plants, R_f (see equation (7)) stands for the foliage costs of all plants, R_r (see equation (14)) are the root costs of all plants summed over all soil layers, and R_v (see equation (20)) are the costs associated with the vascular systems of all plants combined.

3.5. Optimization Strategy

[45] The optimizable vegetation properties (or "degrees of freedom") were divided into properties that are adapted in the short term and respond to the day-to-day changes in environmental conditions, and those properties that are assumed to be adapted to the long-term environmental conditions at the site. Below, we will describe which vegetation properties were optimized for the long term and which were optimized day-by-day.

3.5.1. Long-Term Optimization: $M_{A,p}$, $y_{r,p}$, and Water Use

[46] The long-term adaptation was simulated by running the model over a period of 30 years and searching for the optimal vegetation properties that would maximize N_{CP} over that period. The choice of 30 years for the optimization was made in an attempt to consider the necessity for perennial vegetation to survive exceptionally bad years and its adaptation to slow climatic trends possibly contained in the meteorological data. Death of the perennial vegetation was assumed if the tree water store (M_q, section 3.3.1) decreased below 90% of the tree water storage capacity (M_{qx}) in the model [*Schymanski et al.*, 2008b]. In such a case, the vegetation was not considered suitable for the given environment and N_{CP} was set to 0.

[47] The vegetation properties to be optimized over the long term were represented by a small number of invariant parameters in order to limit the uncertainty in the numerical optimization result, while accounting for all the degrees of freedom considered important for the vegetation's adaptation to its environment. The number of optimizable parameters were kept small, because the complexity of the problem and the uncertainty about finding the global optimum increases with each degree of freedom. We used the Shuffled Complex Evolution (SCE) algorithm [*Duan et al.*, 1993, 1994] to find the optimal values for the invariant parameters that would maximize N_{CP} over 30 years. The algorithm is based on a synthesis of several concepts developed for global optimization, and basically performs a search of the parameter space for the optimal parameter values that would satisfy the objective function. The algorithm and its implementation are described in more detail by *Schymanski* [2007, Appendix 3.5].

[48] Water use (transpiration) can be limited either by stomatal conductance or by root water uptake. However, for achieving maximum net carbon profit with a limited amount of water, transpiration should be controlled by stomata in such a way that the slope between CO_2 uptake and transpiration is maintained as constant during a day [*Cowan and Farquhar*, 1977; *Cowan*, 1982, 1986; *Schymanski et al.*, 2008a]. This slope will be called λ_s and λ_p for seasonal and perennial plants respectively. Over longer time periods, the parameters λ_s and λ_p should be sensitive to the availability of soil water and this sensitivity could be seen as a plant physiological response shaped by evolution to suit a given environment [*Cowan and Farquhar*, 1977]. In the present study, the sensitivity of λ_s and λ_p to soil water was parameterized as:

$$\lambda_s = c_{\lambda f,s} \left(\sum_{i=1}^{i_{r,s}} h_i \right)^{c_{\lambda e,s}} \tag{22}$$

and

$$\lambda_p = c_{\lambda f,p} \left(\sum_{i=1}^{i_{r,p}} h_i \right)^{c_{\lambda e,p}} \tag{23}$$

where $i_{r,s}$ and $i_{r,p}$ denote the deepest soil layer accessed by roots of seasonal and perennial plants respectively.

Equations (22) and (23) are aimed at allowing the largest possible flexibility for the relationship between soil water and λ_s or λ_p while using the least possible number of adjustable parameters. The above formulations include only two adjustable parameters for each relationship ($c_{\lambda f}$ and $c_{\lambda e}$) and allow for relationships ranging from constant λ ($c_{\lambda e}$ = 0) through to linear relationships ($c_{\lambda e}$ = 1.0) and to highly nonlinear relationships ($c_{\lambda e} \gg 1.0$ or $c_{\lambda e} \ll 0$). Soil water availability was represented by the suction head in the rooting zone, because we expected that plants would more likely be able to "sense" the suction head than the total amount of water available in their rooting zones.

[49] In summary, long-term adaptation of vegetation to the environment was modeled by the optimization of six parameters: $M_{A,p}$, $y_{r,p}$, $c_{\lambda f,p}$, $c_{\lambda e,p}$, $c_{\lambda f,s}$ and $c_{\lambda e,s}$.

3.5.2. Daily Optimization: $M_{A,s}$, J_{max25}, and Root Distributions

[50] The fraction occupied by seasonal vegetation ($M_{A,s}$) and the electron transport capacities of seasonal and perennial vegetation ($J_{max25,s}$ and $J_{max25,p}$ respectively) can change dynamically and have a direct impact on photosynthetic rates ($A_{g,s}$, $A_{g,p}$) and daily net carbon profit (N_{CPd}, mol m^{-2} d^{-1}). Their dynamic adaptation to the environment was modeled at a daily scale, by computing N_{CPd} for each day using three different values for each variable, the simulated values for that day and alternative values taken as a specified increment higher and lower (see below). The values for $M_{A,s}$, $J_{max25,s}$ and $J_{max25,p}$ on the subsequent day were then set to the combination of values that would have led to the largest N_{CPd} on the previous day. The daily increment had to be small enough to prevent oscillation between two highly nonoptimal states under stable environmental conditions and large enough to allow a rapid but biologically feasible adaptation to seasonal changes in environmental conditions. This was achieved by setting the daily increment for $M_{A,s}$ to 0.02, while the daily increment for $J_{max25,s}$ and $J_{max25,p}$ was set to 1% of their actual values.

[51] The above parameters and meteorological conditions, in combination with the values of λ_s and λ_p, determine the canopy water demands of seasonal and perennial plants respectively. On the basis of these water demands, the fine root surface area distributions of perennial and seasonal plants ($S_{Ar,p,i}$ and $S_{Ar,i,s}$ respectively) were optimized separately at a daily scale to allow adequate root water uptake with the lowest possible total root surface area. The optimization was performed following the procedure described by *Schymanski et al.* [2008b], where the reader can also find a discussion of the simulated fine root dynamics compared with field observations.

3.6. Study Site

[52] The model presented in this study optimizes vegetation for given environmental conditions, which consist of long-term meteorological data (solar irradiance, vapor pressure, air temperature, rainfall) and catchment properties (catchment geometry and soil type). To compare model results with observations, we chose a test site for which long-term observations of vegetation and canopy-scale water and CO_2 fluxes were available.

3.6.1. Physical Site Properties

[53] The site chosen for the present study is located in the Northern Territory of Australia, 35 km southeast of Darwin, near Howard Springs in the Howard River catchment. A flux tower recording meteorological data and fluxes of CO_2 and water vapor was located at 12°29′39.30″S, 131°9′8.58″E.

[54] The climate is subhumid on an annual basis (1750 mm mean annual rainfall, 2300 mm mean annual class A pan evaporation), but with a very strong monsoonal seasonality. Approximately 95% of the 1750 mm mean annual rainfall is restricted to the wet season (December to March, inclusive), while the dry season (May to September) is characterized by virtually no rainfall and high atmospheric water demand [*Hutley et al.*, 2000]. In general, the availability of water is highest at the site when atmospheric water demand is low (daytime relative humidity >60% during the wet season), and lowest when the atmospheric water demand is high (daytime relative humidity 10–40% during the dry season). Air temperatures range between roughly 25 and 35°C in the wet season and between 15 and 30°C in the dry season.

[55] Daily shortwave radiation during the dry season is between 15 and 25 MJ m^{-2} d^{-1}, while during the wet season it varies between 5 and 30 MJ m^{-2} d^{-1}. The larger day-to-day variation during the wet season is due to the higher variability in cloud cover.

[56] The terrain at the study site is very flat, with slopes <1° [*Beringer et al.*, 2003]. The surface of the lowland plains, where the study site is situated, is a late Tertiary depositional surface, with a sediment mantle that seldom reaches more than 30 to 40 m in depth. Because of the pronounced climatic seasonality, the surface has been intensively weathered, resulting in a lateritic profile, with infertile, acidic soils [*Russell-Smith et al.*, 1995]. At the study site itself, the soil profile has been described as a red kandosol, with sandy loams and sandy clay loams in horizons A and B respectively and weathered laterite in the C horizon, below about 1.2 m [*Kelley*, 2002].

[57] The site is situated between the Howard River (4.5 km to the west, around 20 m AHD (Australian Height Datum)) and a smaller river channel (0.5 km to the East, around 30 m AHD). The terrain reaches a maximum elevation of roughly 40 m AHD between these two channels. In terms of the catchment conceptualization for the water balance model [*Schymanski et al.*, 2008b], we interpreted the catchment as having an average depth of the pedosphere (Z) of 15 m, and an average channel elevation (z_r) of 10 m from the reference datum, which was set to coincide with the average bedrock elevation, so that z_s = 0 m).

3.6.2. Vegetation

[58] The vegetation has been classified as a Eucalypt open forest [*Specht*, 1981], with a mean canopy height of 15 m, where the overstorey has an estimated cover of 50% [*Hutley et al.*, 2000] and is dominated by the evergreen *Eucalyptus miniata* and *E. tetrodonta*. Visual estimates of projected tree cover by analysis of cast shadows in June 2005 suggested values closer to 30% than 50%. This is also confirmed by estimates of projected cover derived from remote sensing [after *Donohue et al.*, 2008, Figure 7]. The dominant tree species contribute to 60–70% of the total basal area (i.e., the ground area covered by tree trunks) of this forest and are accompanied by some brevideciduous, semideciduous and fully deciduous tree species [*O'Grady et al.*, 2000].

[59] The understorey at the site is highly dynamic. During the dry season it is composed of immature (suckers)

individuals of overstorey tree species, some fully or partly deciduous shrubs and some perennial grasses with a total LAI of around 0.2, while during the wet season it is dominated by up to 2 m tall annual C_4 grasses of the genus *Sarga sp.* and reaches LAI values of 1.5 [*Beringer et al.*, 2007].

[60] The root system of the vegetation at the site is mainly limited to the top 4–5 m of soil [*Kelley*, 2002], with single roots observed at depths of up to 9 m, but not in significant quantities (A. P. O'Grady, unpublished data, 1996).

[61] The most significant disturbances affecting vegetation at the site are fires in 2 out of 3 years and severe cyclones every 40–50 years. The population and size structure of the trees at the site indicates that the vegetation may still be recovering from destruction caused by Cyclone Tracy in 1974 [*O'Grady et al.*, 2000]. Bush fires of low to moderate intensity [*Beringer et al.*, 2003] occur more frequently at the study site, with generally less permanent damage than severe cyclones. Since the establishment of the eddy flux tower in 2001, the site has been burnt every year around July or August. However, it has been shown that CO_2 fluxes recovered within a few weeks from the fires that occurred during the observation period [*Beringer et al.*, 2003, 2007; *Schymanski et al.*, 2007].

3.7. Flux Measurements

[62] The measurement techniques used at the site are described in detail elsewhere [*Beringer et al.*, 2003, 2007; *Hutley et al.*, 2005] and will only be summarized here. The present study site is the one described as a "moderate intensity site" with respect to the fire regime given by *Beringer et al.* [2003].

[63] Flux measurements were conducted at the top of an 23 m tower over the 12–14 m tall canopy, in a flat terrain (slopes <1°) with a near homogeneous fetch of more than 1 km in all directions. The eddy covariance technique was used to calculate vertical fluxes of latent heat and CO_2 from three dimensional wind velocities and turbulent fluctuations of CO_2 and H_2O in the air. Soil moisture was measured using Time Domain Reflectometry (TDR) type probes (Campbell Scientific CS616) at 10 cm depth and soil temperature was obtained from soil averaging thermocouple sensors at 2 and 6 cm depth (Campbell Scientific TCAV). All flux variables were sampled at 20 Hz and averaged over 30 minutes. Measurements have been made since 2001. To ensure a continuous data set, small gaps (less than 2 h) were filled using linear interpolation, while larger gaps were filled using a neural network model fitted to the whole data set [*Beringer et al.*, 2007]. Periods with gap-filled data were flagged for later recognition.

3.8. Atmospheric Forcing

[64] Although local meteorological and flux measurements were only available for the period 2001 to 2005, the model was run for 30 years, between 1976 and 2005, in order to model acclimation of the vegetation to the long-term environmental conditions. Meteorological data for this period was obtained from the Queensland Department of Natural Resources, Mines and Water (SILO Data Drill, http://www.nrm.qld.gov.au/silo). The original data set contained, among others, daily totals of global solar radiation, precipitation, daily maxima and minima of air temperature and daily values of atmospheric vapor pressure, all of which were obtained by interpolation of data from the nearest measurement stations and/or estimation based on proxy data. The methodology used for the compilation of the data set is described by *Jeffrey et al.* [2001]. The data was interpolated to the location 12°30′S, 131°09′E and was expected to capture the general trends and cross correlations between different meteorological variables at the site. To run the vegetation optimality model, the daily data had to be transformed into diurnal data, especially solar irradiance, temperature and atmospheric water vapor deficit. This procedure is described in Appendix A.

3.9. Conversion of Measured Fluxes

[65] The on-site eddy covariance measurements delivered half-hourly averages of latent heat flux (in W m^{-2}) and net CO_2 flux (in mg CO_2 s^{-1} m^{-2}). Latent heat flux is the result of all water vapor moving past the sensors and accounts for transpiration, evaporation from the soil and wet surfaces and potential sinks due to the formation of dew. Net CO_2 flux represents a sum of all processes within the system, which either take up or release CO_2. The only significant process that leads to CO_2 uptake on this site is photosynthesis, while CO_2 release occurs through the respiration of leaves, sapwood and roots, as well as soil decomposition processes.

[66] The optimality model used here predicts only foliage gas exchange due to leaf photosynthesis and leaf respiration (lumped in the variable $A_{g,tot}$), transpiration (E_t) and soil evaporation ($E_{su} + E_{ss}$). In order to make valid comparisons between modeled and measured fluxes, we needed to extract the relevant parts from the measured bulk fluxes. This was performed following the procedure outlined in Appendix B.

[67] The relative magnitudes of the different components of the net carbon flux are shown in Figure 4, with reversed signs for F_{nC} and $A_{g,tot}$ to achieve greater clarity.

4. Results

[68] The model was run for 30 years between 1976 and 2005 and forced by rainfall, solar radiation, atmospheric vapor pressure deficit and air temperature. N_{CP} was maximized for the whole period of 30 years, and the last 4 years of the modeled fluxes were compared against observations. The sensitivity of the optimized parameters to the unknown water transport cost parameter c_{rv} was assessed by running the optimization for values of c_{rv} ranging between 0.9 and 1.5×10^{-6} mol m^{-3} s^{-1}. For each value of c_{rv}, the optimization was repeated four times to check for the reliability of the optimization procedure. The results are summarized in Figure 5. The projected cover of perennial vegetation ($M_{A,p}$) turned out to be most sensitive to the value of c_{rv}, and most robust between model runs with the same c_{rv} (Figure 5e). The optimal rooting depth responded similarly to c_{rv} but with a lower sensitivity. The water use parameters in Figures 5a–5d were less sensitive to c_{rv} but displayed clear differences between seasonal and perennial vegetation components (Figures 5a and 5b versus Figures 5c and 5d). The simulated water and CO_2 fluxes were also sensitive to the choice of c_{rv}, as shown in Figure 6, whereby some of the decrease in transpiration (Figure 5b) was negated by a concurrent increase in soil evaporation (Figure 5c) with increasing c_{rv}.

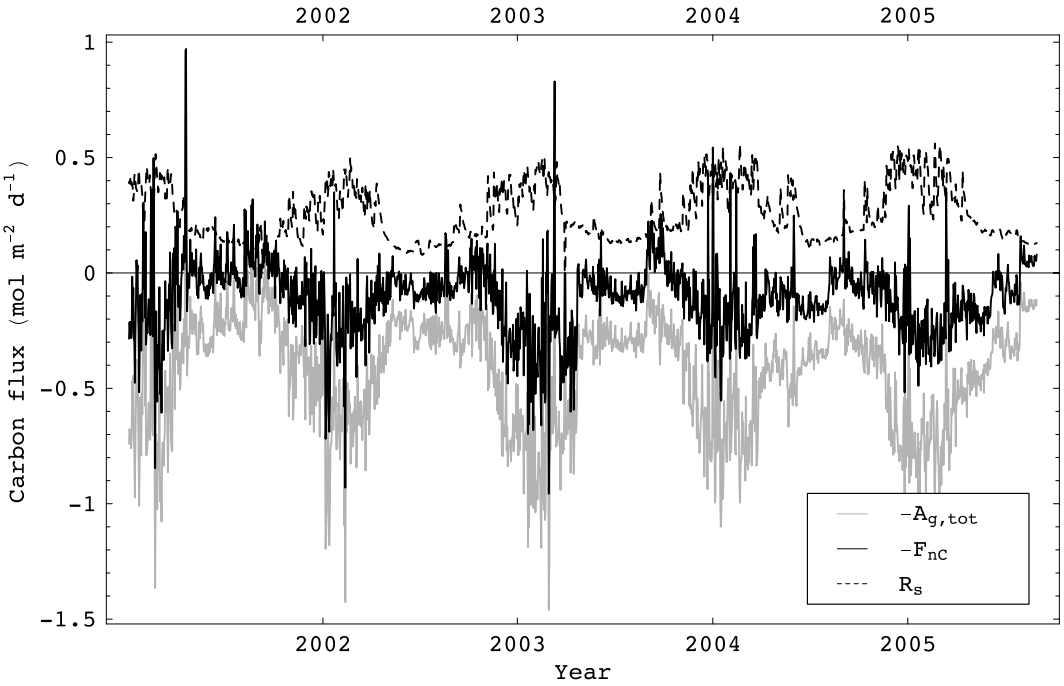

Figure 4. Subdivision of measured net ecosystem CO_2 uptake (F_{nC}, solid black line) into soil respiration (R_s, dashed line), foliage CO_2 uptake ($A_{g,tot}$, solid grey line), and woody tissue respiration (R_w, not shown). R_s and R_w are modeled on the basis of measurements, while A_g is taken as the sum of F_{nC}, R_s, and R_w. For clarity, all fluxes have been plotted as negative values for carbon uptake and positive values for carbon release (note the signs in the legend).

[69] Figure 5 identifies the value of $c_{rv} = 1.2 \times 10^{-6}$ mol m^{-3} s^{-1} as the best choice to reproduce the estimated tree canopy cover of 30% and rooting depth of 4–5 m (Figure 5e). The following analysis will refer to the simulation results obtained with the parameter set that achieved the highest N_{CP} for $c_{rv} = 1.2 \times 10^{-6}$ mol m^{-3} s^{-1}. The achieved N_{CP} was 2650.28 mol m^{-2} in 30 years, while the optimal parameter values were $c_{\lambda f,s} = 726.7$, $c_{\lambda e,s} = -1.03$, $c_{\lambda f,p} = 2174.4$ and $c_{\lambda e,p} = -0.20$ for the water use parameters and $M_{A,p} = 0.336$ and $y_{r,p} = 4.5$ m for the fractional cover and rooting depth of perennial vegetation respectively.

[70] The seasonal vegetation cover ($M_{A,s}$) varied between 0 in the dry season and 0.664 in the wet season, adding up to a total vegetation cover of $M_{A,s} + M_{A,p} = 1.0$ in the wet season (Figure 7b). The resulting modeled rates of evapotranspiration (E_T) and CO_2 uptake ($A_{g,tot}$) agreed well with the observed rates in the period for which observations were available (Figure 8). During this period, mean annual observed E_T was 1182 mm, and mean annual modeled E_T was 1228 mm. $A_{g,tot}$ was overestimated by the model during the wet to dry season transitions in 2002, 2004 and 2005, leading to a slight overprediction of annual CO_2 uptake during the plotted period, with a simulated average of 184 mol m^{-2} a^{-1} compared with the observed average of 159 mol m^{-2} a^{-1} (Figure 8).

[71] The daily optimized J_{max25} expressed annual cycles with maxima during the dry seasons for the perennial plants ($J_{max25,p}$) and during the wet seasons for seasonal plants ($J_{max25,s}$, Figure 7a). The simulated time series of $J_{max25,p}$ seemed to follow the annual cycle of solar irradiance, while the simulated time series of $J_{max25,s}$ followed a seasonal pattern similar to M_A (Figure 7b). During the wet seasons, when M_A is at its maximum value, the simulated values for $J_{max25,p}$ and $J_{max25,s}$ largely coincide. The drop in both $J_{max25,s}$ and M_A during the dry seasons is likely a result of lack of water within the shallow rooting zone of the seasonal plants. Note that the simulated seasonality and dry season magnitudes of M_A corresponded well with satellite-derived (AVHRR) estimates of fractional foliage cover [*Donohue et al.*, 2008], but the wet season values of M_A were 50% higher than the satellite-derived values (Figure 7b). The AVHRR pixel used was 1 km^2 and averaged over the landscape. On a landscape basis, inspections of high-resolution satellite imagery (Spot Image and QuickBird in Google Earth) revealed that about 30% of the landscape was composed of seasonal lagoons, which would lead to a corresponding reduction in the satellite-derived value of fractional foliage cover (T. McVicar, personal communication, 2008). A quantitative correction for the standing water in the pixel is not possible with the available data, but it is obvious that removing the 30% of the area covered by standing water would result in an estimate of up to 100% in the rest of the pixel, which would be consistent with the simulated M_A.

[72] The physiological water use parameters λ_s (seasonal plants) and λ_p (perennial plants) were both positively correlated with the inverse of the average suction head (m) in their respective rooting zones ($c_{\lambda f,s} = 727$ and $c_{\lambda e,s} = -1.0$ in equation (22) and $c_{\lambda f,p} = 2174$ and $c_{\lambda e,p} = -0.20$ in equation (23). This led to similar values for both λ_s and λ_p during the wet season, but a much faster decline of λ_s at the end of each wet season compared with the slow decline of λ_p (Figure 7c). At the shorter time scale, λ_s was also much

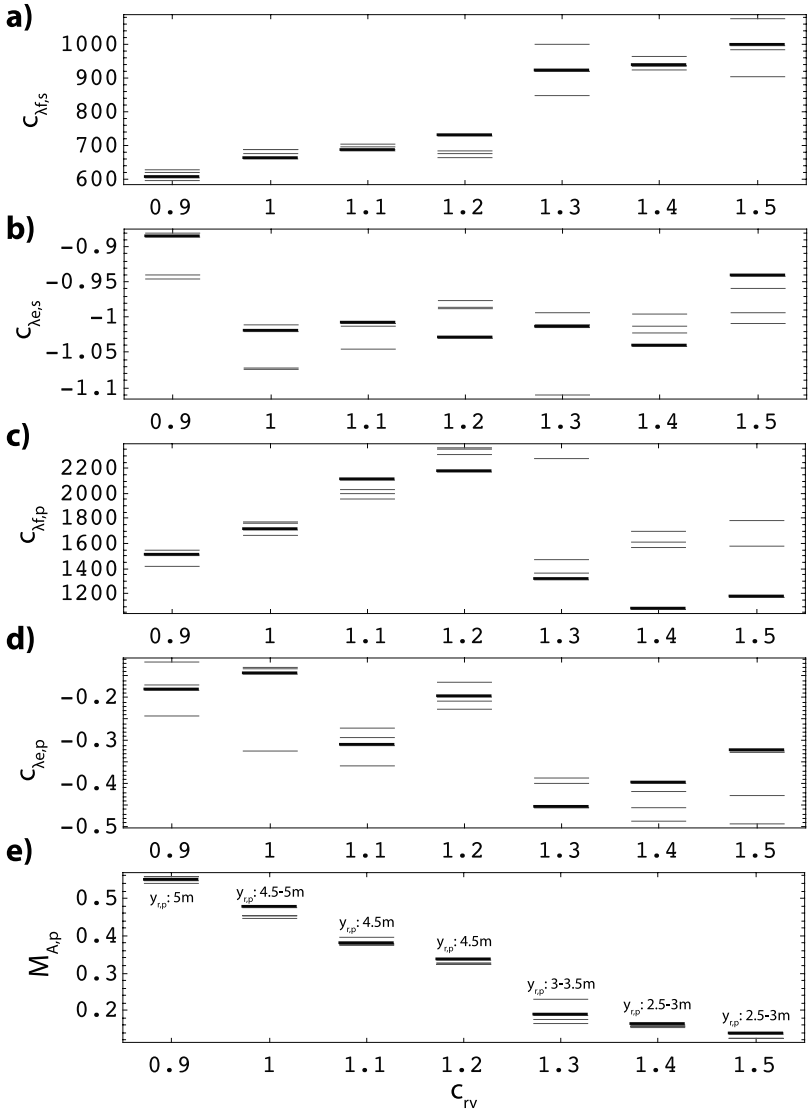

Figure 5. Sensitivity of the optimized parameters to the value of c_{rv}. Each column illustrates the optimal parameter values from four model runs, where the run with the highest N_{CP} is marked in bold. (a–d) Parameters defining the sensitivity of the water use parameters λ_s and λ_p to soil moisture. (e) Optimal fractional cover and rooting depth of perennial vegetation ($M_{A,p}$ and $y_{r,p}$ respectively).

more responsive to pulses of rainfall than λ_p (Figures 7c and 7d).

5. Discussion

[73] The aim of this study was to construct and test a model of transpiration by natural vegetation that would not require any knowledge about the local vegetation at a site or any parameter fitting to match the results with observations. Given that the value for the cost parameter c_{rv} (equation (20)) had to be tuned to give reasonable results, the reader might conclude that the authors have not succeeded. However, it is remarkable that the ''right'' choice of only this one parameter value and the maximization of N_{CP} resulted in reasonable time series of evapotranspiration (E_T), CO_2 uptake ($A_{g,tot}$) and seasonal vegetation cover ($M_{A,s}$), as well as reasonable values for perennial vegetation cover ($M_{A,p}$) and rooting depth ($y_{r,p}$). To our knowledge, the presented model is the first one to simulate the dynamics of water and carbon fluxes as well as vegetation properties without calibration against the observed time series or vegetation-type-specific parameterization. Note that the maximization of N_{CP} led to a fairly constrained range of the optimized parameters (Figure 5), which would not be the case if some of the traditional objective functions were employed. For example, the results arising from objective functions such as maximization of E_T or gross primary productivity (equivalent to A_g+R_l), or the minimization of stress, if implemented in the presented model, can be deduced intuitively. For the first case, stomatal conductivity and fine root surface area would tend to infinity, for the second case, photosynthetic capacity (J_{max25}) would tend to infinity and for the last case, E_t would tend to 0. Given the vast range of possible results that could be produced by the presented model if the N_{CP}

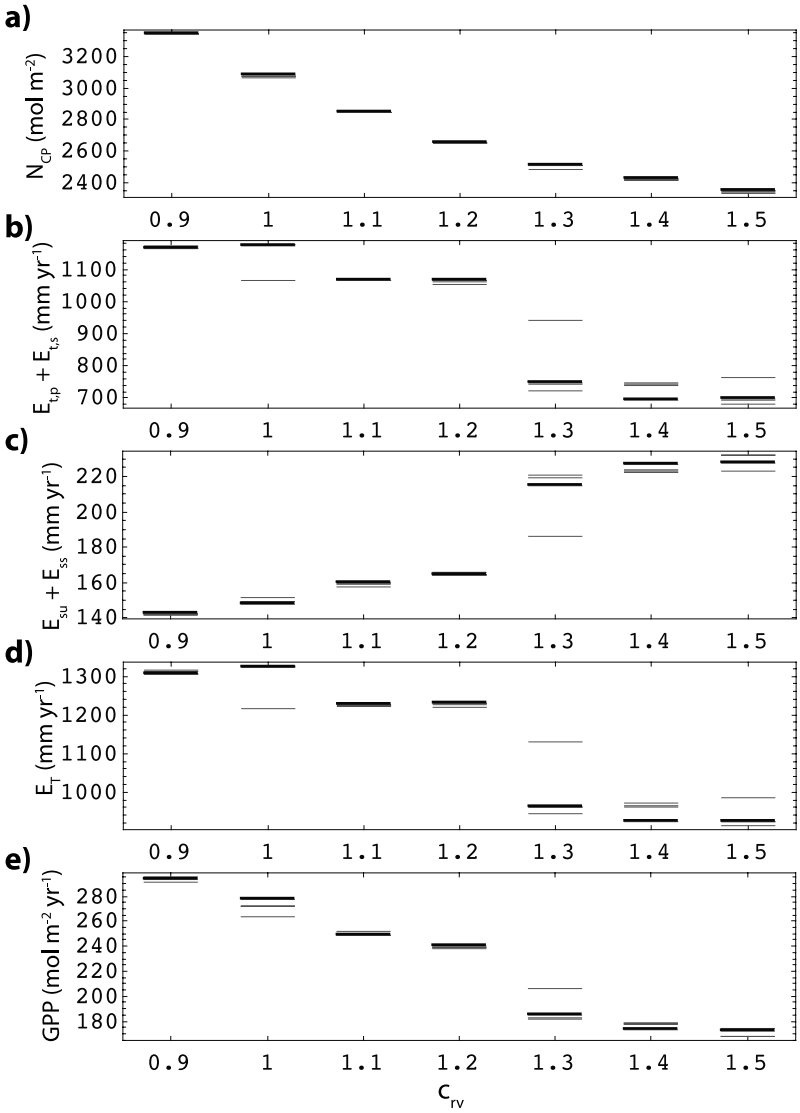

Figure 6. Sensitivity of the achieved net carbon profit and simulated fluxes to the value of c_{rv}. Each column illustrates the results from four model runs, where the run with the highest N_{CP} is marked in bold. (a) Total net carbon profit achieved over 30 years. (b) Simulated mean annual transpiration. (c) Simulated mean annual soil evaporation. (d) Simulated mean annual evapotranspiration. (e) Simulated mean annual gross primary production ($A_{g,s} + R_{l,s} + A_{g,p} + R_{l,p}$).

were not maximized, we conclude that the approximate fit to observations obtained as a result of maximising N_{CP} implicates maximum N_{CP} as a governing principle for ecological adaptation.

[74] The carbon costs of the vascular system (R_v) of the perennial vegetation, resulting from the choice of the cost parameter c_{rv}, would be equivalent to a constant carbon loss of 1.6 μmol s^{-1} m^{-2}. As pointed out in Appendix B, the aboveground woody tissue respiration observed at the site is equivalent to 0.78 μmol s^{-1} m^{-2} [*Cernusak et al.*, 2006]. Considering a 1:1 partitioning between aboveground and belowground carbon allocation as a first estimate, we would estimate the total carbon costs of the vascular system at the site as $0.78 \times 2 = 1.56$ μmol s^{-1} m^{-2}, which is very close to the 1.6 μmol s^{-1} m^{-2} given by the model. The remaining question is whether the chosen value of c_{rv} is a universal constant valid for a wide range of conditions and vegetation types, or whether it is likely to depend on, for example, soil type or other environmental conditions. This will be tested in a follow-up study, where the model will be applied to a range of catchments in different climates, using the same value of c_{rv} throughout.

[75] Other slight inconsistencies with the claim that no knowledge about the local vegetation was needed for the model are the parameterization of the temperature dependence of $J_{\max}$, which was obtained from measurements on eucalypts and the parameterization of M_d and M_{qx} in section 3.3.1, which was derived from observations at the site. However, we found that these parameterizations did not have a great impact on the results [see also *Schymanski et al.*, 2008b] for the effects of M_d and M_{qx}), and only served as estimates of reasonable relationships in the absence of knowledge about the costs and benefits of temperature adaptation and water storage tissues.

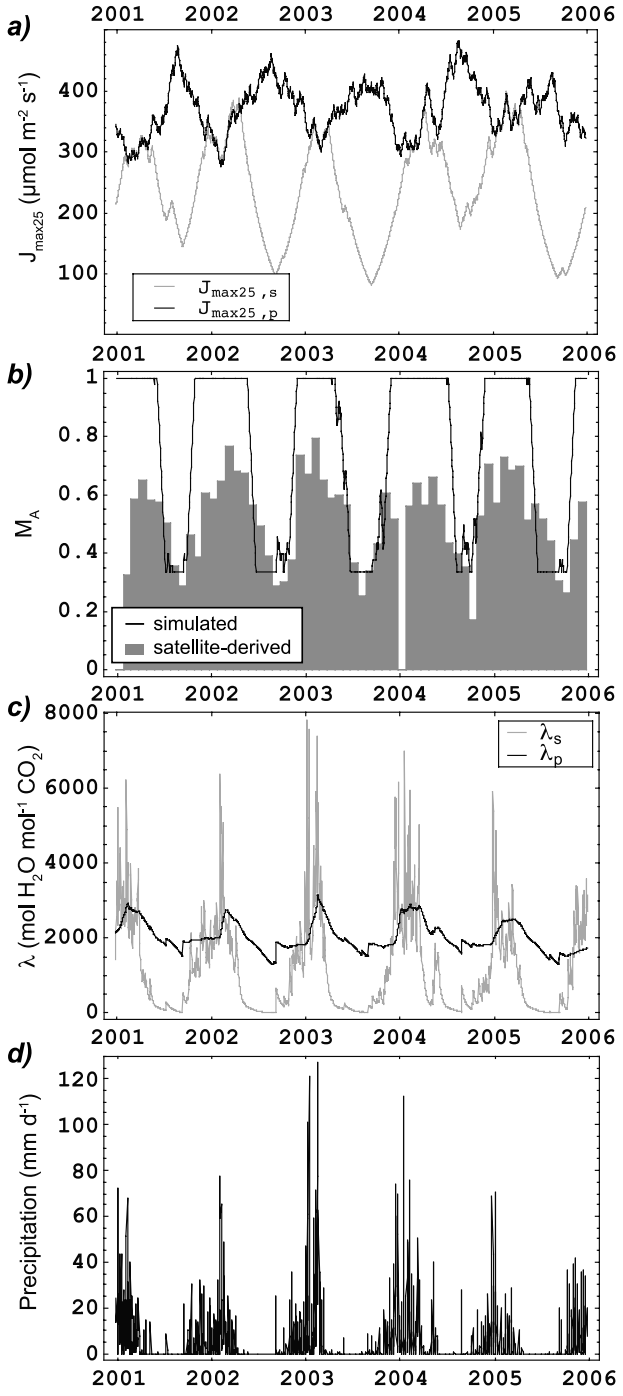

Figure 7. Simulated seasonal dynamics in canopy properties and observed rainfall between 2001 and 2005. (a) Electron transport capacity (J_{max25}) of the seasonal and perennial components ($J_{max25,s}$ and $J_{max25,p}$, respectively), (b) area fraction covered by vegetation compared with satellite-derived estimates [*Donohue et al.*, 2008], (c) slopes between E_t and A_g for the seasonal and perennial components (λ_s and λ_p, respectively), and (d) observed daily rainfall. Note that the satellite-derived data include flooded areas during the wet season.

[76] The present model suggests that most of the vegetation dynamics at the site can be captured by subdividing the vegetation into only two components, a perennial component, which has to be adapted to withstand the severest conditions experienced at the site, and a seasonal component, which is very flexible and makes use of the best conditions at the site. This is consistent with investigations by *Eamus et al.* [2000], who found that dry season conditions determine the wet season water use by trees. However, the assumption that the seasonal vegetation component is only composed of grasses with shallow root systems is probably not applicable to vegetation types where deciduous trees play a significant role. Further differentiation of various vegetation components might be necessary for broader application of the model. For example, deciduous trees could be represented by a third "big leaf" with optimized invariant rooting depth and area fraction, but variable leaf area. Another caveat is that the model does not consider the necessity of seasonal vegetation to complete a full life cycle before it senesces. Therefore, it simulated short pulses of growth after singular rainfall events during the dry season, which were not observed at the site (e.g., years 2002 and 2004 in Figure 7b). On the other hand, the model simulated a longer perseverance of the seasonal plants at the end of the wet seasons in 2002, 2004 and 2005, leading to increased rates of modeled $A_{g,tot}$ compared with the observed values in Figure 8. This is probably because the annual grasses at the site have evolved to complete their life cycle within a short wet season (e.g., 2003 in Figure 8) and cannot take advantage of prolonged favorable conditions after seeds have been produced.

[77] The simulated slope between A_g and E_t for trees (λ_p) was higher during the wet seasons than during the dry seasons (Figure 7). This is not consistent with the results obtained using a previous multilayer canopy model, which suggested that the vegetation on this site operated at higher values of λ in July and October 2004 (around 5000 mol mol^{-1}) compared with January and February 2005 (around 1500 mol mol^{-1}) [*Schymanski et al.*, 2008a]. It was hypothesized in that study that the trees at the site generally operated at a higher value of λ than the grasses, leading to a shift in the effective λ between the wet and the dry season that was related to the seasonality in grass cover. This is not reflected in the present study, as the simulated λ_p does not exceed values of around 3000 mol mol^{-1}. We believe that the lower values of λ_p simulated in this study are caused by the big-leaf simplification. This simplification is expected to lead to an overestimation of the electron transport rates particularly under clear sky conditions, because the big-leaf model is not able to capture the effect of shading within the canopy. An overestimation of J_e under the prevalently clear sky conditions during the dry season would lead to the same E_t at a lower value of λ_p, which is obvious in the work by *Schymanski et al.* [2008a, Figure 1]. While the big-leaf simplification did not seem to have a large influence on the simulated fluxes, it did have an influence on the simulated values of λ, hence these values have to be treated with caution. However, the fact that the optimal combinations of J_{max} and λ reproduced the observed fluxes despite the simplifications suggests that the optimality approach is capable of evening out moderate errors in process param-

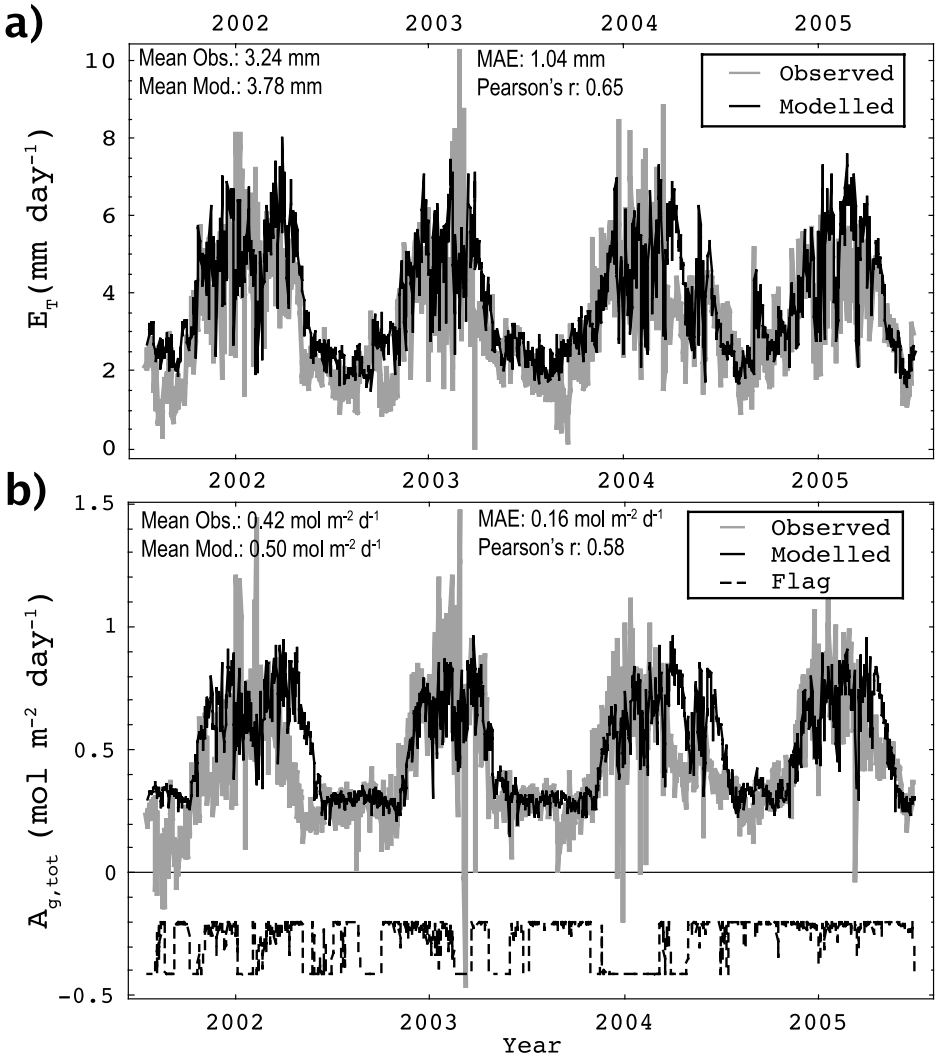

Figure 8. Modeled (black) and observed (grey) daily (a) evapotranspiration rates (E_T) and (b) net CO_2 assimilation rates ($A_{g,tot}$). The dashed line shows scaled daily averages of the validity flag values, ranging from −0.2 for a whole day of valid measurements to −0.4 for a whole day of gap-filled data using a neural network approach. The plots also display the means of the time series as well as the mean absolute errors (MAE) and Pearson's r values of the simulations.

eterization as long as the costs and benefits of the optimized parameters are correct.

6. Conclusions

[78] Maximization of the N_{CP} is a possible principle for self-organization of plant communities. The objective function of maximizing N_{CP} of the whole vegetation at the site led to the emergence of vegetation properties and CO_2 uptake rates in the model, which were consistent with observations. Since only one constant (c_{rv}) was tuned, it is unlikely that the tuning would have compensated for a wrong model structure or unrealistic assumptions about the objective function and optimized vegetation properties.

[79] Costs associated with water transport may be responsible for the reduced perennial vegetation cover. Realistic predictions of the seasonality in grass cover and the total surface area fraction covered by the deeper rooting trees were only achieved if the carbon costs related to water transport tissues were parameterized appropriately (Figure 5e). Without consideration of these costs, optimal vegetation cover using our approach would be 100% throughout the year [*Schymanski et al.*, 2007].

[80] If rooting costs are derived from the feedback between vegetation water use and the catchment water balance, vegetation optimality allows modeling of water and CO_2 fluxes and some key vegetation properties from day to day and from year to year without a priori assumptions about the vegetation at a particular site. The coupling of a physical water balance model with the vegetation optimality model allowed realistic predictions of the dynamics of water and carbon fluxes as well as some key vegetation properties over many years without calibration and without prescription of the local vegetation type. This is, in our view, a sensational achievement, as it will potentially allow predicting vegetation properties and water use in ungauged catchments and under long-term climate change scenarios. In addition, the model could potentially

be used to predict properties of the "potential natural vegetation" at sites where this cannot be achieved using observations of remnant vegetation. Predictions regarding the magnitude and seasonality of transpiration obtained from the model could further be used as input to more sophisticated runoff models that suffer from uncertainty in the estimation of the transpiration component.

Appendix A: Transformation of Daily Data Into Diurnal Data

[81] To run the vegetation optimality model, the daily data had to be transformed into diurnal data, especially solar irradiance, temperature and atmospheric water vapor deficit. The mole fraction of CO_2 in the air was assumed to be invariant at 0.00035 mol mol^{-1} and daily rainfall was distributed evenly over 24 h.

[82] The diurnal variation in global irradiance (I_g) was estimated from the solar elevation angle (β) and daily global irradiance ($I_{g,d}$), after *Spitters et al.* [1986]:

$$I_g = \sin(\beta(t))\frac{I_{g,d}}{\int \sin(\beta(t))dt} \tag{A1}$$

where β is a function of time and the integral includes all daylight hours. The solution of this equation is given by *Schymanski* [2007, Appendix A.3.4.2].

[83] The diurnal variation in air temperature (T_a) was expressed as a function of daily mean temperature ($T_{a,m}$) and daily temperature range ($T_{a,r}$) [*Bilbao et al.*, 2002]:

$$\begin{aligned} T_a = T_{a,m} + T_{a,r}(&0.4632\cos(c_h - 3.805) \\ &+ 0.0984\cos(2c_h - 0.360) \\ &+ 0.0168\cos(3c_h - 0.822) \\ &+ 0.0138\cos(4c_h - 3.513)) \end{aligned} \tag{A2}$$

where all temperatures are expressed in K and c_h changes with the hour of the day (t_h) [*Bilbao et al.*, 2002]:

$$c_h = \frac{1}{12}\pi(t_h - 1) \tag{A3}$$

Atmospheric vapor deficit (D_v) was defined as the difference between the partial pressure of water vapor in air (p_{va}) and saturation vapor pressure (p_{vsat}), divided by air pressure (P_a, set to 101325 Pa):

$$D_v = \frac{p_{vsat} - p_{va}}{P_a} \tag{A4}$$

The vapor pressure (p_{va}) given in the meteorological database was assumed to be constant during the day, so that the diurnal variation in D_v was expressed as a result of the diurnal variation in saturation vapor pressure (p_{vsat}), which was calculated using the common approximation [*Allen et al.*, 1998]:

$$p_{vsat} = 610.8e^{\frac{17.27(T_a-273)}{T_a-35.7}} \tag{A5}$$

where p_{vsat} has units of Pa and T_a is given in units of K.

Appendix B: Conversion of Measured Fluxes

[84] We assumed that modeled transpiration by perennial and seasonal plants ($E_{t,p}$ and $E_{t,s}$ respectively) and soil evaporation combined are equivalent to the latent heat flux estimated using the eddy covariance technique, and lumped all into "evapotranspiration" (E_T):

$$E_T = E_{ss} + E_{su} + E_{t,p} + E_{t,s} \tag{B1}$$

where $E_{t,p}$ and $E_{t,s}$ were converted from molar units (mol s^{-1} m^{-2}) to volumetric units of liquid water (m^3 m^{-2} s^{-1} = m s^{-1}), using the molar weight of water (0.018 kg mol^{-1}) and the density of water (set to 1000 kg m^{-3}).

[85] The measured CO_2 uptake by the soil-vegetation system (F_{nC}, mol m^2 s^{-1}) was subdivided conceptually into net CO_2 uptake by foliage ($A_{g,tot}$, mol m^2 s^{-1}), CO_2 release by soil respiration (R_s, mol m^2 s^{-1}) and CO_2 release by sapwood respiration (R_w, mol m^2 s^{-1}).

$$F_{nC} = A_{g,tot} - R_s - R_w \tag{B2}$$

Soil respiration rates were estimated using a model formulated for an African savanna [*Hanan et al.*, 1998], after setting the "critical temperature" in that model to the maximum soil temperature recorded in our data set (44.95°C) and the intrinsic soil respiration rate at 20°C to 1.86 μmol s^{-1} m^{-2}. The estimated soil respiration rates corresponded well with point measurements at our study site [*Chen et al.*, 2002; *Schymanski*, 2007].

[86] Aboveground woody tissue respiration (R_w) has been measured at the site by *Cernusak et al.* [2006] and estimated to be around 297 g C m^{-2} ground area a^{-1}, which is equivalent to 0.78 μmol s^{-1} m^{-2} or 0.8 g C m^{-2} d^{-1}, averaged over the whole year. No clear seasonal variation was identified, so we took this value as a constant over the whole period.

[87] **Acknowledgments.** We thank Nigel Tapper for his support in the data acquisition; Erik Veneklaas, Sandra Berry, and Tom Buckley for helpful discussions and literature references; Yoshiyuki Yokoo, Neil Viney, Haksu Lee, Majid Hassanizadeh, Miko Kirschbaum, and Richard Silberstein for helpful advice on various modeling issues; and Emma Schymanski for critical review of the manuscript. We would also like to thank Paolo D'Odorico, Kelly Caylor, Ryan Emanuel, and an anonymous referee for constructive comments that helped improve the final manuscript. The research was funded by the Department for Education, Science and Training, Canberra, and the Cooperative Research Centre for Greenhouse Accounting.

References

Allen, R. G., L. S. Pereira, D. Raes, and M. Smith (1998), Crop evapotranspiration—Guidelines for computing crop water requirements, *Irrig. and Drainage Pap.*, *56*, Food and Agric. Organ., U. N., Rome.

Badeck, F. (1995), Intra-leaf gradient of assimilation rate and optimal allocation of canopy nitrogen: A model on the implications of the use of homogeneous assimilation functions, *Funct. Plant Biol.*, *22*(3), 425–439.

Beringer, J., L. B. Hutley, N. J. Tapper, A. Coutts, A. Kerley, and A. P. OGrady (2003), Fire impacts on surface heat, moisture and carbon fluxes from a tropical savanna in northern Australia, *Int. J. Wildland Fire*, *12*(3–4), 333–340.

Beringer, J., L. B. Hutley, N. J. Tapper, and L. A. Cernusak (2007), Savanna fires and their impact on net ecosystem productivity in North Australia, *Global Change Biol.*, *13*, 990–1004, doi:10.1111/j.1365-2486.2007.01334.x.

Bilbao, J., A. H. de Miguel, and H. D. Kambezidis (2002), Air temperature model evaluation in the north Mediterranean belt area, *J. Appl. Meteorol.*, *41*(8), 872–884.

Buckley, T. N., and D. W. Roberts (2006), Despot, a process-based tree growth model that allocates carbon to maximize carbon gain, *Tree Physiol.*, *26*(2), 129–144.

Canny, M. J., and C. X. Huang (2006), Leaf water content and palisade cell size, *New Phytol.*, *170*(1), 75–85.

Caylor, K. K., T. M. Scanlon, and I. Rodriguez-Iturbe (2004), Feasible optimality of vegetation patterns in river basins, *Geophys. Res. Lett.*, *31*, L13502, doi:10.1029/2004GL020260.

Caylor, K. K., P. DOdorico, and I. Rodriguez-Iturbe (2006), On the ecohydrology of structurally heterogeneous semiarid landscapes, *Water Resour. Res.*, *42*, W07424, doi:10.1029/2005WR004683.

Cernusak, L., L. B. Hutley, J. Beringer, and N. J. Tapper (2006), Stem and leaf gas exchange and their responses to fire in a north Australian tropical savanna, *Plant Cell Environ.*, *29*(4), 632–646.

Chen, X. Y., D. Eamus, and L. B. Hutley (2002), Seasonal patterns of soil carbon dioxide efflux from a wet-dry tropical savanna of northern Australia, *Aust. J. Bot.*, *50*(1), 43–51.

Collins, D. B. G., and R. L. Bras (2007), Plant rooting strategies in water-limited ecosystems, *Water Resour. Res.*, *43*, W06407, doi:10.1029/2006WR005541.

Cowan, I. R. (1982), Regulation of water use in relation to carbon gain in higher plants, in *Physical Plant Ecology II*, *Enyclopedia of Plant Physiology*, *12 B*, edited by O. Lange et al., 589–613, Springer, Berlin.

Cowan, I. R. (1986), Economics of carbon fixation in higher plants, in *On the Economy of Plant Form and Function*, edited by T. J. Givnish, pp. 133–171, Cambridge Univ. Press, Cambridge, U. K.

Cowan, I. R., and G. D. Farquhar (1977), Stomatal function in relation to leaf metabolism and environment, in *Integration of Activity in the Higher Plant*, edited by D. H. Jennings, pp. 471–505, Cambridge Univ. Press, Cambridge, U. K.

de Pury, D. G. G., and G. D. Farquhar (1997), Simple scaling of photosynthesis from leaves to canopies without the errors of big-leaf models, *Plant Cell Environ.*, *20*(5), 537–557.

Dewar, R. (1996), The correlation between plant growth and intercepted radiation: An interpretation in terms of optimal plant nitrogen content, *Ann. Bot.*, *78*(1), 125–136.

Dewar, R. C. (2000), A model of the coupling between respiration, active processes and passive transport, *Ann. Bot.*, *86*(2), 279–286.

Donohue, R. J., M. L. Roderick, and T. R. McVicar (2008), Deriving consistent long-term vegetation information from avhrr reflectance data using a cover-triangle-based framework, *Remote Sens. Environ.*, *112*(6), 2938–2949, doi:10.1016/j.rse.2008.02.008.

Duan, Q. Y., V. K. Gupta, and S. Sorooshian (1993), Shuffled complex evolution approach for effective and efficient global minimization, *J. Optim. Theory Appl.*, *76*(3), 501–521.

Duan, Q. Y., S. Sorooshian, and V. K. Gupta (1994), Optimal use of the SCE-UA global optimization method for calibrating watershed models, *J. Hydrol.*, *158*(3–4), 265–284.

Eagleson, P. S. (1978), Climate, soil, and vegetation: 6. Dynamics of the annual water balance, *Water Resour. Res.*, *14*(5), 749–764.

Eagleson, P. S. (1982), Ecological optimality in water-limited natural soil-vegetation systems: 1. Theory and hypothesis, *Water Resour. Res.*, *18*(2), 325–340.

Eamus, D., A. P. O'Grady, and L. B. Hutley (2000), Dry season conditions determine wet season water use in the wet-dry tropical savannas of northern Australia, *Tree Physiol.*, *20*(18), 1219–1226.

Eissenstat, D. M., and R. D. Yanai (1997), The ecology of root lifespan, *Adv. Ecol. Res.*, *27*, 1–60.

Eissenstat, D. M., C. E. Wells, R. D. Yanai, and J. L. Whitbeck (2000), Building roots in a changing environment: Implications for root longevity, *New Phytol.*, *147*(1), 33–42.

Evans, J. R. (1993), Photosynthetic acclimation and nitrogen partitioning within a lucerne canopy. 2. Stability through time and comparison with a theoretical optimum, *Aust. J. Plant Physiol.*, *20*(1), 69–82.

Farquhar, G. D., T. N. Buckley, and J. M. Miller (2002), Optimal stomatal control in relation to leaf area and nitrogen content, *Silva Fennica*, *36*(3), 625–637.

Givnish, T. J. (1988), Adaptation to sun and shade—A whole-plant perspective, *Aust. J. Plant Physiol.*, *15*(1–2), 63–92.

Guswa, A. J. (2008), The influence of climate on root depth: A carbon cost-benefit analysis, *Water Resour. Res.*, *44*, W02427, doi:10.1029/2007WR006384.

Hanan, N. P., P. Kabat, A. J. Dolman, and J. A. Elbers (1998), Photosynthesis and carbon balance of a Sahelian fallow savanna, *Global Change Biol.*, *4*(5), 523–538.

Hikosaka, K. (2003), A model of dynamics of leaves and nitrogen in a plant canopy: An integration of canopy photosynthesis, leaf life span, and nitrogen use efficiency, *Am. Nat.*, *162*(2), 149–164.

Hutley, L. B., A. P. OGrady, and D. Eamus (2000), Evapotranspiration from eucalypt open-forest savanna of northern Australia, *Funct. Ecol.*, *14*(2), 183–194.

Hutley, L. B., R. Leuning, J. Beringer, and H. A. Cleugh (2005), The utility of the eddy covariance techniques as a tool in carbon accounting: Tropical savanna as a case study, *Aust. J. Bot.*, *53*(7), 663–675.

Jeffrey, S. J., J. O. Carter, K. B. Moodie, and A. R. Beswick (2001), Using spatial interpolation to construct a comprehensive archive of Australian climate data, *Environ. Modell. Softw.*, *16*(4), 309–330.

Kelley, G. (2002), Tree water use and soil water dynamics in savannas of northern Australia, Ph.D. thesis, Northern Territory Univ., Darwin, Northern Territory, Australia.

Kerkhoff, A. J., S. N. Martens, and B. Milne (2004), An ecological evaluation of Eaglesons optimality hypotheses, *Funct. Ecol.*, *18*, 404–413.

Kleidon, A., and M. Heimann (1996), Simulating root carbon storage with a coupled carbon-water cycle root model, *Phys. Chem. Earth*, *21*(5–6), 499–502.

Kleidon, A., and M. Heimann (1998), A method of determining rooting depth from a terrestrial biosphere model and its impacts on the global water and carbon cycle, *Global Change Biol.*, *4*(3), 275–286.

Laio, F., P. D'Odorico, and L. Ridolfi (2006), An analytical model to relate the vertical root distribution to climate and soil properties, *Geophys. Res. Lett.*, *33*, L18401, doi:10.1029/2006GL027331.

Medlyn, B. E., et al. (2002), Temperature response of parameters of a biochemically based model of photosynthesis. II. A review of experimental data, *Plant Cell Environ.*, *25*(9), 1167–1179.

O'Grady, A. P., X. Chen, D. Eamus, and L. B. Hutley (2000), Composition, leaf area index and standing biomass of eucalypt open forests near Darwin in the Northern Territory, Australia, *Aust. J. Bot.*, *48*(5), 629–638.

Porporato, A., F. Laio, L. Ridolfi, and I. Rodriguez-Iturbe (2001), Plants in water-controlled ecosystems: Active role in hydrologic processes and response to water stress—III. Vegetation water stress, *Adv. Water Resour.*, *24(7), 725–744.*

Radcliffe, D. E., and T. C. Rasmussen (2002), Soil water movement, in *Soil Physics Companion*, edited by A. W. Warrick, pp. 85–126, CRC Press, Boca Raton, Fla.

Raupach, M. R. (2005), Dynamics and optimality in coupled terrestrial energy, water, carbon and nutrient cycles, in *Predictions in Ungauged Basins: International Perspectives on State of the Art and Pathways Forward*, edited by S. W. Franks et al., *IAHS Publ.*, *301*, 223–238.

Reggiani, P., M. Sivapalan, and S. M. Hassanizadeh (2000), Conservation equations governing hillslope responses: Exploring the physical basis of water balance, *Water Resour. Res.*, *36*(7), 1845–1863.

Roderick, M. L., and M. J. Canny (2005), A mechanical interpretation of pressure chamber measurements—What does the strength of the squeeze tell us?, *Plant Physiol. Biochem.*, *43*(4), 323–336.

Rodriguez-Iturbe, I., P. D'Odorico, A. Porporato, and L. Ridolfi (1999a), On the spatial and temporal links between vegetation, climate, and soil moisture, *Water Resour. Res.*, *35*(12), 3709–3722.

Rodriguez-Iturbe, I., P. D'Odorico, A. Porporato, and L. Ridolfi (1999b), Tree-grass coexistence in savannas: The role of spatial dynamics and climate fluctuations, *Geophys. Res. Lett.*, *26*(2), 247–250.

Roxburgh, S. H., S. L. Berry, T. N. Buckley, B. Barnes, and M. L. Roderick (2005), What is NPP? Inconsistent accounting of respiratory fluxes in the definition of net primary production, *Funct. Ecol.*, *19*(3), 378–382.

Russell-Smith, J., S. Needham, and J. Brock (1995), The physical environment, in *Kakadu: Natural and Cultural Heritage and Management*, edited by T. Press et al., pp. 94–126, Aust. Nat. Conserv. Agency, Darwin, Northern Territory, Australia.

Schenk, H. J. (2005), Vertical vegetation structure below ground: Scaling from root to globe, *Prog. Bot.*, *66*, 341–373.

Schymanski, S. J. (2007), Transpiration as the leak in the carbon factory: A model of self-optimising vegetation, Ph.D. thesis, Univ. of W. Aust., Perth, West. Aust., Australia.

Schymanski, S. J., M. L. Roderick, M. Sivapalan, L. B. Hutley, and J. Beringer (2007), A test of the optimality approach to modelling canopy properties and CO_2 uptake by natural vegetation, *Plant Cell Environ.*, *30*(12), 1586–1598, doi:10.1111/j.1365-3040.2007.01728.x.

Schymanski, S. J., M. L. Roderick, M. Sivapalan, L. B. Hutley, and J. Beringer (2008a), A canopy scale test of the optimal water use hypothesis, *Plant Cell Environ.*, *31*, 97–111, doi:10.1111/j.1365-3040.2007.01740.x.

Schymanski, S. J., M. Sivapalan, M. L. Roderick, J. Beringer, and L. B. Hutley (2008b), An optimality-based model of the coupled soil moisture and root dynamics, *Hydrol. Earth Syst. Sci.*, *12*(3), 913–932.

Simunek, J., M. T. van Genuchten, and M. Sejna (2005), The HYDRUS-1D software package for simulating the one-dimensional movement of water,

heat, and multiple solutes in variably-saturated media, technical report, version 3.0, Dep. of Environ. Sci., Univ. of Calif., Riverside.

Specht, R. L. (1981), Foliage projective cover and standing biomass, in *Vegetation Classification in Australia*, edited by A. N. Gillison and D. J. Anderson, pp. 10–21, Commonw. Sci. and Indust. Res. Organ., Canberra, A.C.T., Australia.

Spitters, C. J. T., H. A. J. M. Toussaint, and J. Goudriaan (1986), Separating the diffuse and direct component of global radiation and its implications for modeling canopy photosynthesis. 1. Components of incoming radiation, *Agric. For. Meteorol.*, *38*(1–3), 217–229.

van der Tol, C., A. J. Dolman, M. J. Waterloo, and A. G. C. A. Meesters (2008a), Optimum vegetation characteristics, assimilation, and transpiration during a dry season: 2. Model evaluation, *Water Resour. Res.*, *44*, W03422, doi:10.1029/2007WR006243.

van der Tol, C., A. G. C. A. Meesters, A. J. Dolman, and M. J. Waterloo (2008b), Optimum vegetation characteristics, assimilation, and transpiration during a dry season: 1. Model description, *Water Resour. Res.*, *44*, W03421, doi:10.1029/2007WR006241.

van Genuchten, M. T. (1980), A closed-form equation for predicting the hydraulic conductivity of unsaturated soils, *Soil Sci. Soc. Am. J.*, *44*(5), 892–898.

van Wijk, M. T., and W. Bouten (2001), Towards understanding tree root profiles: Simulating hydrologically optimal strategies for root distribution, *Hydrol. Earth Syst. Sci.*, *5*(4), 629–644.

J. Beringer, School of Geography and Environmental Science, Monash University, Clayton, Vic 3800, Australia.

L. B. Hutley, School of Science and Primary Industries, Charles Darwin University, Darwin, NT 0909, Australia.

M. L. Roderick, Environmental Biology Group, Research School of Biological Sciences and Research School of Earth Sciences, Australian National University, GPO Box 475, Canberra, ACT 2601, Australia.

S. J. Schymanski, Max Planck Institute for Biogeochemistry, Postfach 10 01 64, D-07701 Jena, Germany. (sschym@bgc-jena.mpg.de)

M. Sivapalan, Department of Geography, University of Illinois at Urbana-Champaign, Urbana, IL 61801, USA.